ISSN 1063-7788, Physics of Atomic Nuclei, 2018, Vol. 81, No. 6, pp. 945–970. © Pleiades Publishing, Ltd., 2018.

ELEMENTARY PARTICLES AND FIELDS
Theory

# Adiabatic Representation for Atomic Dimers and Trimers in Collinear Configuration*

A. A. Gusev[1)**], S. I. Vinitsky[1),2)], O. Chuluunbaatar[1),3)], A. Góźdź[4)], V. L. Derbov[5)], and P. M. Krassovitskiy[6)]

Received April 17, 2018

**Abstract**—We considered collinear models for a trimer of identical atoms with molecular pair interactions and for an atomic dimer scattered by an atom or tunneling through potential barriers. The models are formulated as 2D boundary-value problems in the Jacobi and polar coordinates. In the adiabatic representation the problems are reduced to a system of second-order ordinary differential equations (SODEs) with respect to the radial variable using the expansion of the desired solutions in the set of angular basis functions that depend on the radial variable as a parameter. The efficiency of the elaborated method, algorithms and programs is demonstrated by benchmark calculations of the asymptotic expansions of basis functions, effective potentials, fundamental solutions of the SODEs, and corresponding asymptotic scattering states, as well as the resonance scattering, metastable and bound states.

**DOI:** 10.1134/S1063778818060169

## 1. INTRODUCTION

At present the resonance scattering of diatomic molecules(dimers) by atoms via three-particle metastable trimer states and the molecular dissociation induced by collisions with atoms are a subject of extensive theoretical and experimental studies [1–5].

To analyze such processes it is conventional to use triatomic model systems with atoms of rare gases bound by pair interactions described, e.g., by realistic molecular and van der Waals potentials, that possess bound and metastable states in the vicinity of the dissociation threshold of the diatomic molecule [6–8]. To extend the class of conventional models we proposed to consider the beryllium dimer [9, 10], in which the bond is covalent in the low-lying (0–4) vibrational energy states and van der Waals in the upper (5–11) states [11, 12], and to investigate the collisions of beryllium dimers with surrounding atoms or the near-surface diffusion [13–15]. Further study of these models and processes stimulates the development and application of the known and new methods and symbolic–numerical algorithms for solving multidimensional boundary-value problems (BVPs) with non-separable variables and the construction of asymptotic states of the triatomic scattering problem below and above the breakup threshold [16–45].

In the present paper, the application of the adiabatic representation to the solution of the above problem is based on the Kantorovich method [46, 47] that provides the required mathematical background, reducing the BVP to a system of the second-order ordinary differential equations (SODEs) with respect to a (hyper)radial variable using the expansion of the desired solutions in a set of angular basis functions, depending on the (hyper)radial variable as a parameter [21, 22, 48], the asymptotic methods [49], and the finite element method (FEM), implemented in the problem-oriented software packages [50–57].

In the present paper we develop the adiabatic representation method in application to the models comprising three particles in the so-called quantum chemistry as a collinear configuration [18]: a trimer of identical atoms with molecular pair interactions and an atomic dimer scattered by an atom or tunneling through short-range potential barriers on a straight line. Then we elaborate algorithms for calculating the asymptotic parametric angular functions, the effective potentials and the fundamental solutions of the SODEs and apply them to the construction of the asymptotic states of the triatomic scattering problem. It is a key problem, because in three-atomic systems

*The text was submitted by the authors in English.

[1)]Joint Institute for Nuclear Research, Dubna, 141980 Russia.
[2)]Peoples' Friendship University of Russia (RUDN University), Moscow, 117198 Russia.
[3)]National University of Mongolia, Ulaanbaatar, Mongolia.
[4)]Institute of Physics, University of M. Curie-Skłodowska, Lublin, Poland.
[5)]Saratov State University, Saratov, Russia.
[6)]Institute of Nuclear Physics, Almaty, Kazakhstan.
**E-mail: gooseff@jinr.ru

at large values of the hyperradial variable the effective potentials of SODEs have the form of expansions in inverse powers of hyperradius even for short-range potentials of pair interactions. Evidently, they should be studied before considering the pair interactions of the van der Waals type. Moreover, in the problem of dimer tunneling above the dissociation threshold, the expansion of the matrix elements of the Gaussian barrier potential begins from the first inverse power of hyperradius, which is equivalent to effective Coulomb repulsion above the threshold. Finally, we test the developed technique by calculating the above asymptotic expansions, the resonance scattering of the atomic dimer by an atom or Gaussian barriers, and the metastable and bound states of a trimer of beryllium atoms below the dissociation threshold.

The paper is organised as follows. In Section 2 we formulate the 2D BVP for the dimer and trimer models. In Section 3 the 2D BVP in polar coordinates is reduced to the SODEs. In Section 4 we present the algorithms and benchmark calculations of the asymptotic behavior of the parametric basis functions and the effective potentials of the ODE system at large values of the radial variable. In Sections 5 and 6 we construct the asymptotic expressions for the fundamental solutions of ODEs and the scattering states. In Sections 7 and 8 we demonstrate the efficiency of the elaborated technique by test calculations of the resonance scattering of an atomic dimer on an atom, the metastable and bound states of a trimer, and the resonance tunneling of a dimer through a Gaussian barrier and the metastable states, respectively. In Conclusion the results and perspectives are discussed.

## 2. SETTING OF THE PROBLEM

Consider a model of three identical particles (trimer) on a straight line with the masses $M_i = M$ and the coordinates $\bar{x}_i \in \mathbf{R}^1$, $i = 1, 2, 3$, of one-dimensional Euclidian space $\mathbf{R}^1$ coupled via the pair short-range potential $\tilde{V}(|\bar{x}_i - \bar{x}_j|)$, $i, j = 1, 2, 3$. Performing the change of variables corresponding to the cyclic permutation $(\alpha, \beta, \gamma) = (1, 2, 3)$ of the permutation group $S_3$ [40]:

$$x_\gamma \equiv x_{(\alpha\beta)} = \bar{x}_\beta - \bar{x}_\alpha,$$
$$y_\gamma \equiv y_{(\alpha\beta)\gamma} = \frac{\bar{x}_\alpha + \bar{x}_\beta - 2\bar{x}_\gamma}{\sqrt{3}},$$
$$x_0 = \frac{\sqrt{2}}{\sqrt{3}}(\bar{x}_1 + \bar{x}_2 + \bar{x}_3),$$

we get three pairs $(x_{(\alpha\beta)}, y_{(\alpha\beta)\gamma})^T$ of the scaled Jacobi variables. In the center-of-mass reference frame of the configuration space $\bar{\mathbf{x}} = (\bar{x}_1, \bar{x}_2, \bar{x}_3) \in \mathbf{R}^3$, i.e., on the hyperplane $\Omega = \{\bar{\mathbf{x}} = (\bar{x}_1, \bar{x}_2, \bar{x}_3) | \bar{x}_1 + \bar{x}_2 + \bar{x}_3 = 0\} \subset \mathbf{R}^3$ (see Fig. 1*a*), these Jacobi maps $(x, y)^T \in \Omega_{xy} \sim \mathbf{R}^2$ are connected by the relations:

$$\begin{pmatrix} x_\gamma \\ y_\gamma \end{pmatrix} \equiv \begin{pmatrix} x_{(\alpha\beta)} \\ y_{(\alpha\beta)\gamma} \end{pmatrix} = \mathbf{T}_{xy}(\varphi_{\gamma\alpha}) \begin{pmatrix} x_\alpha \\ y_\alpha \end{pmatrix},$$
$$\mathbf{T}_{xy}(\varphi_{\gamma\alpha}) = \begin{pmatrix} \cos\varphi_{\gamma\alpha} & \sin\varphi_{\gamma\alpha} \\ -\sin\varphi_{\gamma\alpha} & \cos\varphi_{\gamma\alpha} \end{pmatrix}, \qquad (1)$$

where the angles $\varphi_{\gamma\alpha} = \varphi_{\alpha\beta} = \varphi_{\beta\gamma} = -\varphi_{\alpha\gamma} = -\varphi_{\beta\alpha} = -\varphi_{\gamma\beta} = \frac{2\pi}{3}$, i.e. $\cos\varphi_{\gamma\alpha} = \cos\varphi_{\alpha\beta} = \cos\varphi_{\beta\gamma} = -\frac{1}{2}$, $\sin\varphi_{\gamma\alpha} = \sin\varphi_{\alpha\beta} = \sin\varphi_{\beta\gamma} = \frac{\sqrt{3}}{2}$, are such that $\varphi_{\gamma\alpha} + \varphi_{\alpha\beta} + \varphi_{\beta\gamma} = 2\pi$, $\varphi_{\alpha\gamma} + \varphi_{\beta\alpha} + \varphi_{\gamma\beta} = -2\pi$. With the variable parameter $\varphi$ in $\mathbf{T}_{xy}(\varphi)$ they correspond to a kinematic rotation plus an inversion of O(2) group and simply change the sign of pairs of Jacobi coordinates in Eq. (1),

$$\begin{pmatrix} -x_{(\alpha\beta)} \\ -y_{(\alpha\beta)\gamma} \end{pmatrix} = \mathbf{T}_{xy}(\varphi_{\gamma\alpha} \pm \pi) \begin{pmatrix} x_{(\beta\gamma)} \\ y_{(\beta\gamma)\alpha} \end{pmatrix}. \qquad (2)$$

In Fig. 1*b* the hyperplane $(x, y)^T \in \Omega_{xy}$ is separated by three axes $y_{(12)3}$, $y_{(31)2}$, and $y_{(23)1}$ into six sectors that together with three orthogonal axes $x_{12}$, $x_{31}$, $x_{23}$ describe six channels of the scattering problem for three identical particles. This picture is similar to Fig. 1 for the one-dimensional quantum scattering problem of three particles with pair short-range repulsive potentials [35]. Note that the theorem of existence and uniqueness of the solution of such scattering problem was proved in [36, 37] by constructing the resolvent kernel limit values in the absolutely continuous spectrum. However, the pairs $(y_{(12)3}, x_{12})^T$, $(y_{(31)2}, x_{31})^T$ and $(y_{(23)1}, x_{23})^T$ correspond to the pairs $(l_1, -k_1)^T$, $(l_3, -k_3)^T$, and $(l_2, -k_2)^T$ of Ref. [35]. Our choice is determined by the parameterization of the pairs $(y, x)^T = (\rho\cos\varphi, \rho\sin\varphi)^T$, where the angle $\varphi \in [0, 2\pi)$ is counted counterclockwise from the axis $y_{(12)3}$, for which $\varphi = 0$. This parameterization is more suitable for constructing the asymptotic scattering states at large values of the hyperradius $\rho$ than the conventional one, $(y, x)^T = (\rho\sin\varphi', \rho\cos\varphi')^T$. The kinematic angle $\varphi' \in [-\pi/2, \pi/2]$ corresponds to the double kinematic angle conventionally applied to describe three channels of a three-body scattering problem on half-hyperplane of $\Omega'_{|x||y|} \sim \mathbf{R}^2_+$ enclosed in the six-dimensional configuration space $\mathbf{R}^6 \backslash \{\mathbf{0}\}$ after separating the center-of-mass motion in a three-body system [23, 25].

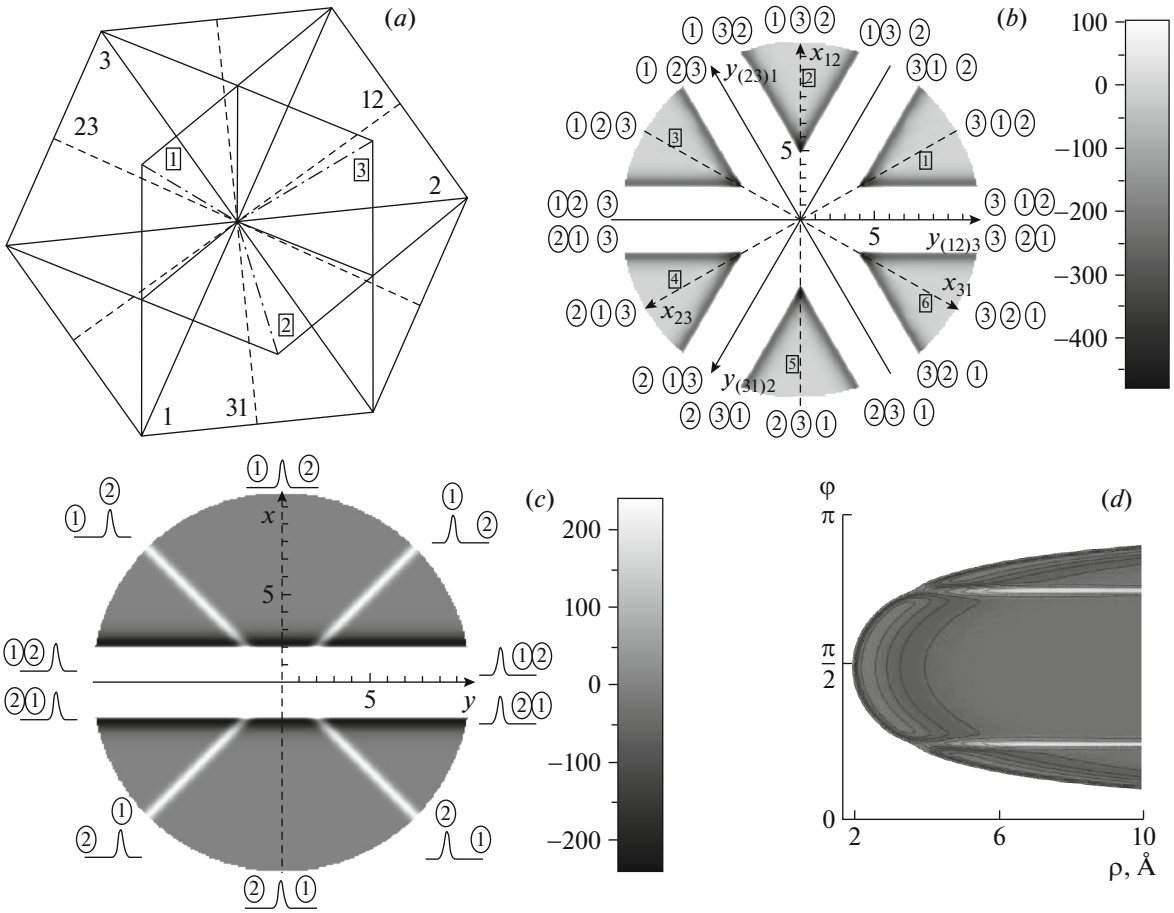


**Fig. 1.** (*a*) The coordinate planes 1, 2, 3, labelled with boxes, the center-of-mass plane in $\mathbf{R}^3$, and the lines of intersection of these planes with the pair-collision planes $x_i = x_j$, corresponding to pair-collision lines $\{x_i = x_j, x_1 + x_2 + x_3 = 0\}$ (labelled 12, 23, 31) in the center-of-mass plane $(x_1, x_2, x_3)|(x_1 + x_2 + x_3 = 0)$, belonging to $\mathbf{R}^2 \subset \mathbf{R}^3$. (*b*) The profiles of 2D potential functions of $Be_3$ trimer in Jacobi coordinates (1) in the center-of-mass plane and the relative arrangement of particles in accordance with the region of the center-of-mass plane. The numbers of sectors are given in boxes. (*c*) The profiles of 2D potential functions of $Be_2$ dimer with barrier and the relative arrangement of particles and barrier. (*d*) The profiles of 2D potential functions of $Be_2$ dimer in one of sectors in polar coordinates. Here coordinates and potential functions are given in Å and $Å^{-2}$, respectively.

As a result, we arrive at the Schrödinger equation for the wave function $\Psi(y, x)$ corresponding to the total energy $E$ of the triatomic system in Jacobi coordinates $(x, y)^T = (x_\gamma, y_\gamma)^T \in \Omega_{xy}$:

$$\left(-\frac{\partial^2}{\partial y^2} - \frac{\partial^2}{\partial x^2} + \frac{M}{\hbar^2}(\tilde{V}(x,y) - \tilde{E})\right) \times \Psi(y,x) = 0. \quad (3)$$

In the case of a diatomic molecule (dimer) with identical nuclei coupled via the pair potential, $\tilde{V}(|\bar{x}_1 - \bar{x}_2|)$, moving in the external potential field $\tilde{V}^b(|\bar{x}_i - \bar{x}_3|)$, $i = 2, 1$, of the third atom having the infinite mass, the same equation (3) is valid for the variables

$$x \equiv x_3 = \bar{x}_2 - \bar{x}_1, \quad y \equiv y_3 = \bar{x}_1 + \bar{x}_2,$$

with respect to the origin of the coordinate frame placed at the infinite-mass atom, $\bar{x}_3 = 0$.

Here the potential function for the trimer with the pair potentials (below this case is referred to as *Task 2*, for example, see Fig. 1*b*),

$$\tilde{V}(x,y) = \tilde{V}(|x|) + \tilde{V}\left(\left|\frac{x - \sqrt{3}y}{2}\right|\right) + \tilde{V}\left(\left|\frac{x + \sqrt{3}y}{2}\right|\right), \quad (4)$$

or the potential function for a dimer in the field of $p$ barrier potential (below this case is referred to as *Task 3*, see Fig. 1*c*)

$$\tilde{V}(x,y) = \tilde{V}(|x|) + \tilde{V}^b\left(\left|\frac{x - y}{2}\right|\right) + \tilde{V}^b\left(\left|\frac{x + y}{2}\right|\right), \quad (5)$$

is an even function with respect to the straight line $x = 0$ (i.e., $\bar{x}_1 = \bar{x}_2$), which allows one to consider the

solutions of the problem in the half-plane $x \geq 0$. The use of the Dirichlet or Neumann boundary condition at $x = 0$ allows one to obtain the solutions, symmetric and antisymmetric with respect to the permutation of two particles. If the pair potential possesses a high peak at the pair collision point, then the solution of the problem in the vicinity of $x = 0$ is exponentially small and can be considered in the half-plane $x \geq x_{\min}$. In this case the Neumann or Dirichlet boundary condition imposed at $x_{\min}$ yields only a minor contribution to the solution. The equation, describing the diatomic molecular subsystem (dimer) (below this case is referred to as *Task 1*), has the form

$$\left(-\frac{d^2}{dx^2} + \frac{M}{\hbar^2}(\tilde{V}(|x|) - \tilde{\varepsilon})\right)\phi(x) = 0. \qquad (6)$$

We assume the energy spectrum of the dimer to consist of the discrete part with a finite number $n_0 \geq 1$ of bound states with the eigenfunctions $\phi_j(x)$, $j = \overline{1, n_0}$ and the eigenvalues $\tilde{\varepsilon}_j = -|\tilde{\varepsilon}_j| < 0$, and the continuous part with the eigenvalues $\tilde{\varepsilon} > 0$ and the corresponding eigenfunctions $\phi_{\tilde{\varepsilon}}(x)$. As a rule, the solutions for the discrete and continuous spectrum of the BVP with Eq. (6) can be found only numerically, except some simplified models having exact solutions and used for computer modelling of bimolecular chemical reactions [58]. In certain cases the eigenfunctions of the continuous spectrum are approximated by the eigenfunctions of pseudostates of the discrete spectrum $\tilde{\varepsilon}_j > 0$, $j = 1 + n_0, \ldots$ calculated in the sufficiently large but finite interval $x \in [x_{\min}, x_{\max}]$ [14].

The approach proposed below is illustrated by the example of $Be_2$ with the reduced mass $M/2 = 4.506$ Da of the nuclei [13, 14] and the molecular interaction approximated by the Morse potential

$$V(x) = \frac{M}{\hbar^2}\tilde{V}(x),$$
$$\tilde{V}(x) = \tilde{D}\{\exp[-2(x - \hat{x}_{eq})\alpha] - 2\exp[-(x - \hat{x}_{eq})\alpha]\}. \qquad (7)$$

Here $\alpha = 2.96812$ Å$^{-1}$ is the potential well width, $\hat{x}_{eq} = 2.47$ Å is the average distance between the nuclei, and $\tilde{D} = 1280$ K, $D = (M/\hbar^2)\tilde{D} = 236.51$ Å$^{-2}$ (1 K $= 0.184766$ Å$^{-2}$, 1 Å$^{-2} = 5.412262$ K) is the potential well depth. This potential supports only five bound states corresponding to the covalent bounding of the $Be_2$ dimer [59] having the energies $\varepsilon_i = (M/\hbar^2)\tilde{\varepsilon}_i$, $i = 1, \ldots, n_0 = 5$, presented in Table 1. The parameter values are determined from the condition $(\tilde{\varepsilon}_2 - \tilde{\varepsilon}_1)/(2\pi\hbar c) = 277.124$ cm$^{-1}$, 1 K$/(2\pi\hbar c) = 0.69503476$ cm$^{-1}$. To solve the discrete spectrum problem we applied the seventh-order FEM using the Hermitian interpolation polynomials with double nodes [57]. As an example, following [13], we use below the Gaussian barrier potentials $V^b(x_i) = D\exp(-x_i^2/\sigma)$ with $D = 236.51$ Å$^{-2}$ and $\sigma = 0.0523$ Å$^2$. The values of parameters of the repulsive Gaussian barrier potential were estimated following the experimental observation of the quantum diffusion of hydrogen atoms on the copper surface [60].

## 3. BOUNDARY-VALUE PROBLEMS

Using the change of variables $x = \rho\sin\varphi$, $y = \rho\cos\varphi$, we rewrite Eq. (3) in polar coordinates $(\rho, \varphi)$, $\Omega_{\rho,\varphi} = (\rho \in (0, \infty), \varphi \in (0, 2\pi))$

$$\left(-\frac{1}{\rho}\frac{\partial}{\partial\rho}\rho\frac{\partial}{\partial\rho} + \frac{1}{\rho^2}\Lambda(\varphi, \rho) - E\right)\Psi(\varphi, \rho) = 0,$$
$$\Lambda(\varphi, \rho) = -\frac{d^2}{d\varphi^2} + \rho^2 V(\varphi, \rho), \qquad (8)$$

where for a trimer with pair potentials

$$V(\varphi, \rho) = V(\rho|\sin\varphi|) + V(\rho|\sin(\varphi - 2\pi/3)|) + V(\rho|\sin(\varphi - 4\pi/3)|), \qquad (9)$$

and for a dimer with pair potential in the external field of barrier potential

$$V(\varphi, \rho) = V(\rho|\sin\varphi|) + V^b(\rho|\sin(\varphi - \pi/4)|) + V^b(\rho|\sin(\varphi + \pi/4)|). \qquad (10)$$

Then in polar coordinates $V^b(\rho|\sin(\varphi \pm \pi/4)|) = D\exp(-\rho^2\sin^2(\varphi \pm \pi/4)/\sigma)$ and $V(\varphi, \rho)$ is displayed in Fig. 1*d*.

The solution of Eq. (8) is sought in the form of the Kantorovich expansion [46, 47]

$$\Psi_{i_o}(\varphi, \rho) = \sum_{j=1}^{j_{\max}} \phi_j(\varphi; \rho)\chi_{ji_o}(\rho). \qquad (11)$$

Here $\chi_{ji_o}(\rho)$ are unknown matrix functions, $j = 1, \ldots, j_{\max} = 2N$. The angular basis functions $\phi_j(\varphi; \rho) \in \mathcal{F}_\rho \sim L_2(\Omega)$ in the interval $\Omega = \varphi \in [0, 2\pi)$, which is divided into $s_{\max}$ subintervals $\Omega_s = \varphi \in (2\pi(s-1)/s_{\max}, 2\pi s/s_{\max})$: $\Omega_{\rho;\varphi} = \bigcup_{s=1}^{s_{\max}} \Omega_s$, are determined at each value of the parameter $\rho \in (0, +\infty)$ as the eigenfunctions corresponding to the real discrete eigenvalues $\varepsilon_1(\rho) < \varepsilon_2(\rho) < \ldots < \varepsilon_j(\rho) < \ldots$ of the Sturm–Liouville problem for the equation

$$(\Lambda(\varphi, \rho) - \varepsilon_j(\rho))\,\phi_j(\varphi; \rho) = 0. \qquad (12)$$

The functions $\phi_j^{(p)}(\varphi; \rho) \equiv \phi_j(\varphi; \rho)$ have the parity $(-1)^p$, $p = 0, 1$ with respect to the inversion of Jacobi coordinates (2), i.e., $\phi_j^{(p)}(\varphi; \rho) = (-1)^p\phi_j^{(p)}(\varphi \pm$

**Table 1.** The discrete spectrum of energies $\varepsilon_i$ of dimer $Be_2$, the total energies $E_\nu$ and the binding energies $E_\nu^B = -(E_\nu - E^a)$ in $Å^{-2}$ of gerade ($g$) and ungerade ($u$) states of trimer $Be_3$ counted of $E^a = \tilde{\varepsilon}_1 = -193.06\,Å^{-2} = -1044$ K dimer energy $Be_2$ calculated in grid $\Omega_\rho = 4.1(20)7(10)10$ at $N = 15$ of Eq. (19) for the trimer models in the configuration space with $d = 2$ and $d = 6$

| $i$ or $\nu$ | $d = 1(3)$ | Even | | | Odd | | |
|---|---|---|---|---|---|---|---|
| | | $d = 2$ | | $d = 6$ | $d = 2$ | | $d = 6$ |
| | $\varepsilon_i$ | $E_\nu^B$ | $E_\nu$ | $E_\nu$ | $E_\nu^B$ | $E_\nu$ | $E_\nu$ |
| 1 | −193.066 | 196.02 | −389.006 | −388.848 | 107.52 | −300.393 | −300.245 |
| 2 | −119.392 | 142.37 | −335.208 | −335.055 | 67.41 | −260.467 | −260.325 |
| 3 | −63.338 | 93.95 | −286.828 | −286.679 | 34.60 | −227.565 | −227.431 |
| 4 | −24.904 | 52.77 | −245.755 | −245.615 | 11.79 | −204.803 | −204.683 |
| 5 | −4.089 | 32.32 | −225.345 | −225.206 | 0.8 | −193.831 | −193.740 |
| 6 | | 22.31 | −215.226 | −215.098 | | | |
| 7 | | 5.14 | −198.129 | −198.020 | | | |

$\pi;\rho)$; here and below $p = 0$. These functions satisfy the orthogonality and completeness conditions

$$\langle\phi_i|\phi_j\rangle = \sum_{s=1}^{s_{\max}} \int_{2\pi(s-1)/s_{\max}}^{2\pi s/s_{\max}} d\varphi\phi_i(\varphi;\rho)\phi_j(\varphi;\rho) = \delta_{ij}, \quad (13)$$

$$\sum_i |\phi_i\rangle\langle\phi_i| = \sum_i \phi_i(\varphi;\rho)\phi_i(\varphi_0;\rho) = \delta(\varphi - \varphi_0). \quad (14)$$

For the three problems under consideration the potential function $V(\varphi,\rho)$ depending on the parameter $\rho$ can be defined as follows.

*Task 1.* The case of one pair potential in the intervals $\varphi \in (0, 2\varphi_\alpha)$ ($\varphi_\alpha = \pi/6$, $\pi/4$ or $\pi/2$) $V(\varphi,\rho) = V(\rho\sin\varphi)$.

*Task 2.* The case of three pair potentials, Eq. (9), in the interval $\varphi \in (0, 2\varphi_\alpha = \pi/3)$; the potential has the symmetry of the $D_{3h}$ dihedral point group [40, 61, 62].

*Task 3.* The case of one pair potential and two penetrable or almost impenetrable barriers, Eq. (10), in the interval $\varphi \in (0, \varphi_\alpha = \pi/2)$ or in the intervals $\varphi \in (0, \varphi_\alpha = \pi/4 - \epsilon)$ and $\varphi \in (\varphi_\alpha = \pi/4 - \epsilon, \pi/2)$, $0 < \epsilon \ll \pi/4$.

The solutions symmetric with respect to the permutation of two particles satisfy the Neumann boundary condition at $\varphi = 0$ and $\varphi = 2\varphi_\alpha$, while the antisymmetric ones satisfy the Dirichlet boundary condition at these points, i.e., at the aforementioned points $x = x_{\alpha\beta} = 0$. If the pair potential possesses a high peak in the vicinity of the pair collision point, then the solution of the problem (8) will be considered in the half-plane $\Omega_{\varphi,\rho} = (\rho \in (\rho_{\min}, \infty), \varphi \in [\varphi_{\min}(\rho), 2\varphi_\alpha - \varphi_{\min}(\rho)])$ with the Neumann or Dirichlet boundary condition. Such approximation corresponds to the so-called hard-core model [24].

The potential function $V(\varphi,\rho)$ of the boundary-value problem (12) is symmetric under the reflection $\hat{I}_\alpha$: $\varphi \to (4s-2)\varphi_\alpha - \varphi$ with respect to the lines $\varphi = (2s-1)\varphi_\alpha$ in each sector of the cycle, numbered by $s = 1, \ldots, s_{\max}$: $\hat{I}_\alpha V(\varphi,\rho) = V(\varphi,\rho)$. Therefore, the set of eigenfunctions $\phi_j(\varphi;\rho)$ is separated into two subsets, namely, the even and odd $\phi_j^{\sigma=\pm1}(\varphi;\rho)$ ones: $\hat{I}_\alpha\phi_j^\sigma(\varphi;\rho) = \phi_j^\sigma((4s-2)\varphi_\alpha - \varphi;\rho) = \pm\phi_j^{\sigma=\pm1}(\varphi;\rho)$. This fact allows separate calculation of *gerade* $\phi_j^g(\varphi;\rho) = \phi_j^g((4s-2)\varphi_\alpha - \varphi;\rho)$ or *ungerade* $\phi_j^u(\varphi;\rho) = -\phi_j^u((4s-2)\varphi_\alpha - \varphi;\rho)$ eigenfunctions in the reduced interval $\varphi \in [\varphi_{\min}(\rho), \varphi_\alpha]$, subjecting them to Neumann or Dirichlet boundary condition at the boundary point $\varphi = \varphi_\alpha$ of the interval, respectively. Below the parametric angular basis functions $\phi_j^{\sigma=\pm1}(\varphi;\rho)$ with the numbers $j = 1, \ldots, n_0$ are referred to as cluster states with $\varepsilon_j(\rho) < 0$, and those with $j \geq n_0 + 1$ as pseudostates with $\varepsilon_j(\rho) > 0$, corresponding to the discrete and continuous spectrum of BVP for Eq. (6) at large values of the parameter $\rho$, respectively. To reveal the above structurization property, we introduce the linear combinations of these functions $\phi_j^{\gamma,\beta}(\varphi;\rho)$ for the trimer and $\phi_j^{\leftarrow,\rightarrow}(\varphi;\rho)$ for the dimer:

$$\phi_j^{\gamma,\beta}(\varphi;\rho)$$

$$= (\pm\phi_j^{\sigma=-1}(\varphi;\rho) + \phi_j^{\sigma=1}(\varphi;\rho))/\sqrt{2},$$
$$\phi_j^{\leftarrow,\rightarrow}(\varphi;\rho)$$
$$= (\pm\phi_j^{\sigma=-1}(\varphi;\rho) + \phi_j^{\sigma=1}(\varphi;\rho))/\sqrt{2}. \quad (15)$$

The action of the parity operator $\hat{I}_\alpha$ on these functions

$$\hat{I}_\alpha\phi_j^\gamma(\varphi;\rho) = \phi_j^\beta(\varphi;\rho), \quad \hat{I}_\alpha\phi_j^\beta(\varphi;\rho) = \phi_j^\gamma(\varphi;\rho),$$
$$\hat{I}_\alpha\phi_j^\leftarrow(\varphi;\rho) = \phi_j^\rightarrow(\varphi;\rho),$$
$$\hat{I}_\alpha\phi_j^\rightarrow(\varphi;\rho) = \phi_j^\leftarrow(\varphi;\rho), \quad (16)$$

consists in the permutation of states $|\gamma\rangle \leftrightarrow |\beta\rangle$ or $|\leftarrow\rangle \leftrightarrow |\rightarrow\rangle$ with respect to the lines $\varphi = (2s-1)\varphi_\alpha$. Indeed, the parametric cluster functions at $j = 1,\ldots,n_0$ and at large $\rho$ have maxima in the vicinity of $\varphi = (2s-2)\varphi_\alpha$ and $\varphi = 2s\varphi_\alpha$, respectively, that correspond to the eigenfunctions of cluster states of the BVP for Eq. (6). In the particular case of sector 1, the dimer functions $\phi_j^{\leftarrow,\rightarrow}(\varphi;\rho)$ have maxima in the vicinity of $\varphi = 0$ and $\varphi = \pi$, i.e. for $y > 0$, $v = \leftarrow$, or for $y < 0$, $v = \rightarrow$ at large $\rho$, respectively while the trimer functions $\phi_j^{\gamma,\beta}(\varphi;\rho)$ have maxima in the vicinity of $\varphi = 0$ and $\varphi = \pi/3$, i.e., for $x_{12}/y_{(12)3} > 0$, $v = \gamma$, or for $x_{31}/y_{(31)2} < 0$ $v = \beta$ at large $\rho$, respectively. The required properties are clearly seen in the plots of even and odd parametric basis functions and their linear combinations (15) of the trimer $Be_3$ (Fig. 2). The first column in Fig. 2 presents the number of the basis function. The second and third columns show the even $\phi_j^g(\varphi;\rho)$ and odd $\phi_j^u(\varphi;\rho)$ basis functions, symmetric and antisymmetric with respect to the straight line $\varphi = \pi/6$, constructed by solving the problem in the interval $\varphi \in [\varphi_{\min}, \pi/6]$ with the Neumann boundary condition at $\varphi = \varphi_{\min}$ and Neumann or Dirichlet boundary condition at $\varphi = \pi/6$, respectively, with subsequent symmetrical extrapolation of the solution into the interval $\varphi \in [\pi/6, \pi/3 - \varphi_{\min}]$. The fourth and fifth columns show the linear combinations of the even and odd functions, which are localized in one of the subdomains for the basis functions ($\phi_j^{g,u}(\varphi;\rho)$, $j = 1,2,3$) below the breakup threshold in contrast to the basis functions ($\phi_j^{g,u}(\varphi;\rho)$, $\phi_j^{g,u}(\varphi;\rho)$, $j = 1,2,3$) above the breakup threshold. Such behavior is typical for angular spheroidal functions [26, 27, 30, 63].

Using the above pairs of the basis functions (15), we rewrite expansion (11) in the $\sigma$ representation

$$\Psi_{i_o}(\varphi,\rho) = \sum_{j=1}^{N}\sum_{\sigma}\phi_j^\sigma(\varphi;\rho)\chi_{ji_o}^\sigma(\rho), \quad (17)$$

where $\sigma = u, g$ or $\sigma = \gamma, \beta$ for the unknown functions $\chi_{ji_o}^\gamma(\rho)$ and $\chi_{ji_o}^\beta(\rho)$ in the $(\gamma\beta)$ representation, related to the functions $\chi_{ji_o}^g(\rho)$ and $\chi_{ji_o}^u(\rho)$ in the $(gu)$ representation as

$$\chi_{ji_o}(\rho) = \begin{pmatrix}\chi_{ji_o}^\gamma(\rho)\\ \chi_{ji_o}^\beta(\rho)\end{pmatrix} = A\begin{pmatrix}\chi_{ji_o}^u(\rho)\\ \chi_{ji_o}^g(\rho)\end{pmatrix},$$
$$A = \frac{1}{\sqrt{2}}\begin{pmatrix}1 & 1\\ -1 & 1\end{pmatrix}. \quad (18)$$

The averaging of Eq. (8) with the basis functions in $\sigma$ representation (17) yields the system of coupled ODEs with the integer $d \geq 1$ determined by the hyperspherical parametrization of the $d$-dimensional configuration space

$$\left[-\frac{1}{\rho^{d-1}}\frac{d}{d\rho}\rho^{d-1}\frac{d}{d\rho} + \frac{\varepsilon_i(\rho)}{\rho^2} - E\right]\chi_{ii_o}(\rho)$$
$$+\sum_{j=1}^{j_{\max}} W_{ij}(\rho)\chi_{ji_o}(\rho) = 0, \quad (19)$$
$$W_{ij}(\rho) = H_{ji}(\rho)$$
$$+\frac{1}{\rho^{d-1}}\frac{d}{d\rho}\rho^{d-1}Q_{ji}(\rho) + Q_{ji}(\rho)\frac{d}{d\rho}, \quad (20)$$

that corresponds to Eq. (8) for $d = 2$ and collinear configuration of three atoms. Here the potential curves (terms) $\varepsilon_j(\rho)$ are eigenvalues of the BVP (12) and the effective potentials (EPs) $Q_{ij}(\rho) = -Q_{ji}(\rho)$, $H_{ij}(\rho) = H_{ji}(\rho)$ are expressed as integrals calculated in the reduced intervals $\varphi \in [0, 2\varphi_\alpha]$ using the above $g, u$ symmetry:

$$Q_{ij}(\rho) = -\langle\phi_i|\partial_\rho\phi_j\rangle,$$
$$H_{ij}(\rho) = \langle\partial_\rho\phi_i|\partial_\rho\phi_j\rangle. \quad (21)$$

For *Task 3* the effective potentials $\hat{W}_{ij}(\rho) = W_{ij}(\rho) + V_{ij}^b(\rho)$ are sums of $W_{ij}(\rho)$, calculated using the potential curves and the parametric basis functions of *Task 1*, and the matrix elements $V_{ij}^b(\rho)$ of the barrier potentials

$$V_{ij}^b(\rho) = \langle\phi_i|V^b(\rho|\sin(\varphi - \pi/4)|)$$
$$+ V^b(\rho|\sin(\varphi + \pi/4)|)|\phi_j\rangle. \quad (22)$$

As an example, we calculated with the required accuracy the parametric basis functions of BVP (12) and the effective potentials (21) for the models of $Be_2$ dimer and $Be_3$ trimer in collinear configuration using the FEM implemented in the program ODPEVP [52]. The results of calculation on the grid $\Omega_\varphi[1.8/\rho, \varphi_\alpha] = \{1.8/\rho(24)3/\rho(10)4/\rho(5)5/\rho(10)\varphi_\alpha\}$ for $\varphi_\alpha = \pi/2$ for $Be_2$ dimer and $\varphi_\alpha = \pi/6$ for $Be_3$ trimer are displayed in Figs. 2, 3, and 4. Using the obtained result in the uncoupled $(gu)$ representation

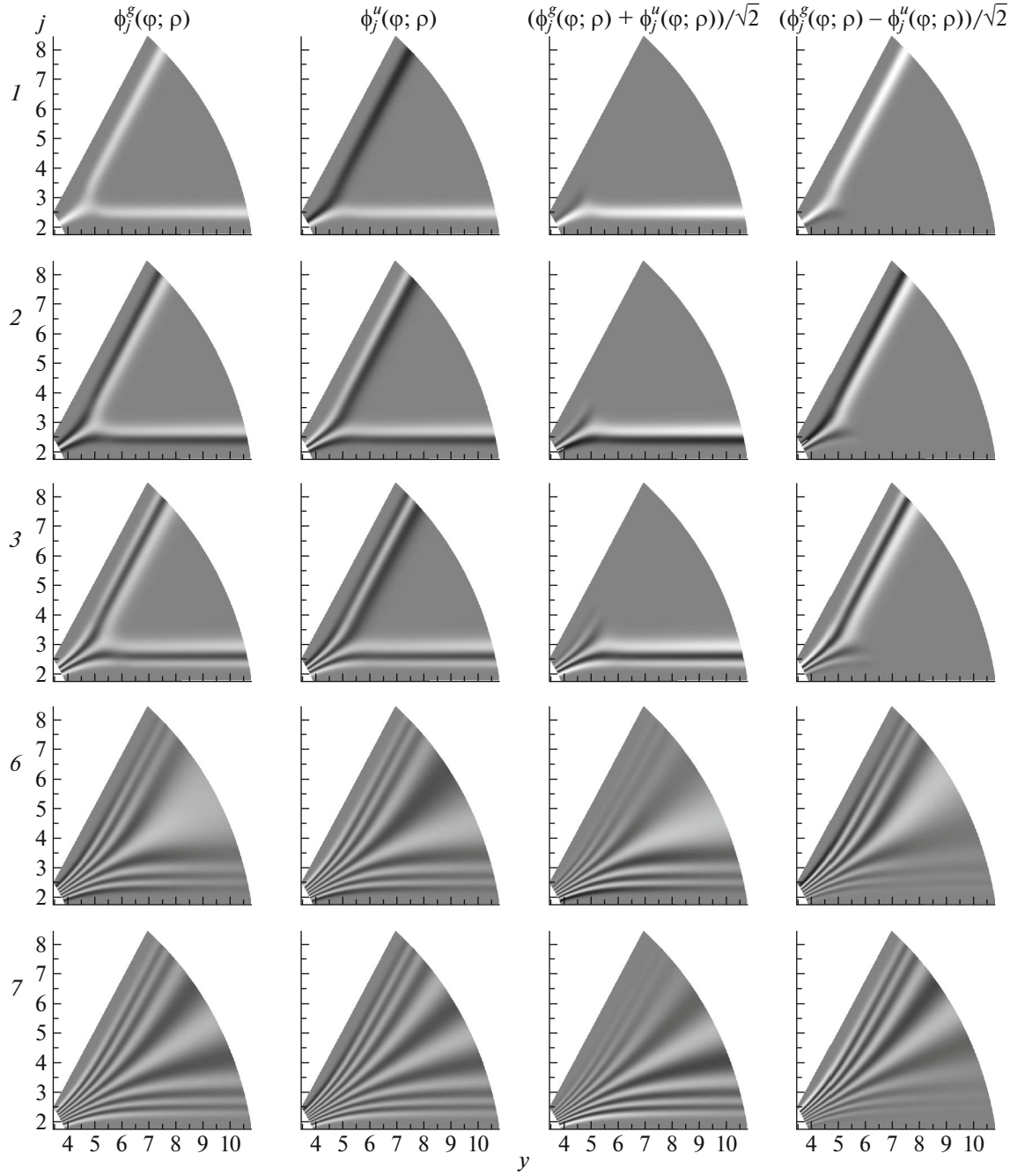


**Fig. 2.** The density plots of the first, second, third, sixth, and seventh basis functions $\phi_j^{g,u}(\varphi;\rho)$, $j = 1, 2, 3, 6, 7$ displayed in sector 1 of $(y, x)$ plane (in Å). The negative, positive, and near-zero values of the eigenfunctions are displayed by black, white, and gray, respectively.

and the transformation matrix $A$ from Eq. (18), we can rewrite the system of ODEs in the coupled $(\alpha\beta)$ representation with the effective potentials expressed similarly [16]

$$U_{ij}(\rho) = \begin{pmatrix} U_{i\gamma j\gamma}(\rho) & U_{i\gamma j\beta}(\rho) \\ U_{i\beta j\gamma}(\rho) & U_{i\beta j\beta}(\rho) \end{pmatrix}$$

$$= A \begin{pmatrix} U_{iuju}(\rho) & 0 \\ 0 & U_{igjg}(\rho) \end{pmatrix} A^{-1}. \qquad (23)$$

In Section 7 one can see that the $(\gamma\beta)$ representation provides the required compatibility of the solutions of Eqs. (19) with the asymptotic boundary conditions (ABCs) of the scattering problem on the total axis $\mathbf{R}^1$ and its semiaxis $\mathbf{R}^1_+$.

*Remark 1.* In collinear configuration both for dimer and for trimer embedded in the configuration space $\mathbf{R}^d\backslash\{\mathbf{0}\}$ at $d = 6$ the BVP for Eq. (8) at $d = 6$ has an upper shift of spectrum in comparison with the spectrum of the BVP for Eq. (8) at $d = 2$ with the corresponding eigenfunctions $\hat{\chi}(\rho)$ expressed in terms of the eigenfunctions $\chi(\rho)$ of Eq. (8) at $d = 2$ by the conventional substitution $\hat{\chi}(\rho) = \rho^{-2}\chi(\rho)$. This fact is confirmed by the comparison of the collinear trimer spectra in the configuration space of dimension $d = 2$ with those in the configuration space of dimension $d = 6$ presented in Table 1. This spectrum shift is due to the additional centrifugal term $(d/2-1)^2\rho^{-2}$ induced by such substitution and the redefinition of fundamental solutions, i.e., the replacement of the zero-index Bessel function $J_0(\sqrt{-E}\rho)$ of Eq. (19) at $W_{ij}(\rho) = 0$ and $d = 2$ with the Bessel function [64] of index two $J_2(\sqrt{-E}\rho)$ at $d = 6$.

## 4. ASYMPTOTIC EXPRESSIONS OF CLUSTER FUNCTIONS

Let us calculate the solution of the Sturm–Liouville problem (12)–(14) at large $\rho$ in domain $x = \rho\sin\varphi \in (0, \rho\sin\varphi_\alpha)$

$$\begin{aligned}&\left(\Lambda(\varphi;\rho) - \varepsilon_j(\rho)\right)\phi_j(\varphi;\rho)\\ &\equiv \left(-\frac{\partial^2}{\partial\varphi^2} + \rho^2\bar{V}(\rho\sin\varphi) - \frac{\varepsilon_j(\rho)}{x_\alpha^2}\right)\\ &\times\phi_j(\varphi;\rho) = 0,\end{aligned} \tag{24}$$

where $\bar{V}(x) = V(x/x_\alpha)/x_\alpha^2$, $x_\alpha = (\pi/2)/\varphi_\alpha$.

Using the new variable $x'$ defined as $\varphi = x'/\rho$, $x' = \rho\arcsin(x/\rho)$, we get

$$\begin{aligned}&\left(-\frac{\partial^2}{\partial x'^2} + \bar{V}(\rho\sin(x'/\rho)) - \frac{\varepsilon_j(\rho)}{\rho^2 x_\alpha^2}\right)\phi_j(x';\rho) = 0,\\ &\phi_j(\varphi_i = x_i'/\rho;\rho) = \sqrt{\rho}\phi_j(x'_i;\rho).\end{aligned} \tag{25}$$

In the argument of the potential function $\bar{V}(\rho\sin(x'/\rho))$ we add and subtract $x'$ and expand it in Taylor series in the vicinity of $x'$,

$$\begin{aligned}\bar{V}(\rho\sin(x'/\rho)) &= \bar{V}(x' + \Delta x')\\ &= \bar{V}(x') + \sum_{k=1}\frac{d^k\bar{V}(x')}{dx'^k}\frac{(\Delta x')^k}{k!},\end{aligned} \tag{26}$$

where a small correction $\Delta x' = \rho\sin(x'/\rho) - x' \ll 1$ is presented again in the form of Taylor series

$$\Delta x' = \sum_{k=1}\frac{(-1)^k}{(2k+1)!}\frac{x'^{2k+1}}{\rho^{2k}}.$$

Then the Sturm–Liouville problem for Eq. (24) is reduced to

$$\begin{aligned}&\left(-\frac{\partial^2}{\partial x'^2} + \bar{V}(x') + \sum_{k=1}\frac{\bar{V}^{(k)}(x')}{\rho^{2k}} - \frac{\varepsilon_j(\rho)}{\rho^2 x_\alpha^2}\right)\\ &\times\phi_j(x';\rho) = 0,\end{aligned} \tag{27}$$

$$\begin{aligned}&\langle\phi_i(\rho)|\phi_j(\rho)\rangle\\ &\equiv \int_{x_0'}^{x'_{\max}} dx'\phi_i(x';\rho)\phi_j(x';\rho) = \delta_{ij}.\end{aligned} \tag{28}$$

Here the first terms $\bar{V}^{(k)}(x')$ of the asymptotic expansion of $\bar{V}(\rho\sin(x'/\rho))$ read as

$$\begin{aligned}\bar{V}^{(1)}(x') &= -\frac{x'^3}{6}\frac{d\bar{V}(x')}{dx'},\\ \bar{V}^{(2)}(x') &= \frac{x'^5}{360}\left(5x'\frac{d^2\bar{V}(x')}{dx'^2} + 3\frac{d\bar{V}(x')}{dx'}\right),\\ \bar{V}^{(3)}(x') &= -\frac{x'^7}{45360}\left(35x'^2\frac{d^3\bar{V}(x')}{dx'^3}\right.\\ &\left.+63x'\frac{d^2\bar{V}(x')}{dx'^2} + 9\frac{d\bar{V}(x')}{dx'}\right),\\ &\dots\end{aligned}$$

Note that $k!\bar{V}^{(k)}(x')$ are the derivatives of the potential of the BVP (27) with respect to the parameter $\rho^{-2}$. So, we apply the modified version of the program ODPEVP [52] for calculating the parameter derivatives of the solution up to the given order to determine the asymptotic expansion of the cluster eigenfunctions and eigenvalues described in detail in Ref. [42].

The execution of the above procedure yields the required asymptotic expansion of the eigenvalues neglecting exchange exponential small terms here and below [49]

$$\begin{aligned}\frac{\varepsilon_j(\rho)}{\rho^2} &= \varepsilon_j^{(0)}(\rho) + \sum_{k=1}^{k_{\max}}\rho^{-2k}\varepsilon_j^{(2k)}\\ &= \lambda_j^{(0)}(\rho) + \sum_{k=1}^{k_{\max}}\frac{\rho^{-2k}}{k!}\lambda_j^{(k)},\end{aligned} \tag{29}$$

where $\varepsilon_j^{(2k)} = \lambda_j^{(k)}/k!$, and of the matrix elements (21) for the cluster states, $i, j = 1, \dots, n_0$:

$$\begin{aligned}Q_{ij}(\rho) &= \sum_{k=1}^{k_{\max}}\frac{Q_{ij}^{(2k-1)}}{\rho^{2k-1}},\\ H_{ij}(\rho) &= \sum_{k=1}^{k_{\max}-1}\frac{H_{ij}^{(2k)}}{\rho^{2k}},\end{aligned}$$

$$V_{ij}(\rho) = O(\exp(-\rho)). \quad (30)$$

For the test beryllium trimer model in collinear configuration, the coefficients $\varepsilon_j^{(k)}$ of expansion (29) and the coefficients $H_{jj}^{(k)}$ of expansion (30) at $i = j$ have been presented in Ref. [42], and the first coefficients of the expansions (30) are given in Appendix. The first six terms of the required asymptotic expansions (29) and (30) at $\rho = 20$ provide the accuracy of 11 significant digits, see Table 2.

*Remark 2.* The effective diagonal potentials (EPs) have the asymptotic expressions $\mathcal{H}_{jj}(\rho) = \varepsilon_j(\rho)\rho^{-2} + H_{jj}(\rho) \approx \varepsilon_j^{(0)} + (\varepsilon_j^{(2)} + H_{jj}^{(2)})\rho^{-2} = \varepsilon_j^{(0)} + (1/4)\rho^{-2}$, proved in Ref. [15] and confirmed in Table 2.

## 5. ASYMPTOTIC EXPRESSIONS OF PSEUDOSTATE FUNCTIONS

Consider the case of $\varphi_\alpha = \pi/2$ illustrated by Fig. 5. The eigenfunctions of pseudostates $\varepsilon_j(\rho)/x_\alpha^2 \geq 0$, $(j - n_0) = 1, 2, \ldots$, are localized beyond the potential well with the $(n_0 - 1)$th node at the potential-well boundary. From this fact an estimate of the eigenvalues for pseudostates $\varepsilon_j(\rho) \approx x_\alpha^2(j - n_0)^2$ follows, namely, the eigenvalues of the corresponding BVPs (27) in the new variable $x'$, $\varepsilon_j = \varepsilon_j(\rho)/\rho^2$, will be small (see Fig. 1*c*). So, the solution $\varepsilon_n(\rho)$ ($\varepsilon_n = \varepsilon_n(\rho)/\rho^2$) of the derived equation is sought in the form of a power series of $g$ and $u$ potential curves at $n = j - n_0$ for $n/\rho < 1$

$$\varepsilon_j(\rho) = x_\alpha^2 \left( n^2 + \sum_{k=1}^{k_{\max}} \frac{\varepsilon_n^{(k)}}{\rho^k} \right). \quad (31)$$

Here and below the $g$ states are numbered by odd $n = 1, 3, \ldots$, and the $u$ states by even $n = 2, 4, \ldots$ Then the numerical values of the function $B(\varphi_i; \rho) = B(x_i')$ and its derivative $B'(\varphi_i; \rho) = \rho B'(x_i')$ on the specified grid $\Omega_\varphi = \{\varphi_1 = \varphi_0, \ldots, \varphi_i = x_i'/\rho, \ldots, \varphi_N = \varphi_\varepsilon\}$ in the polar coordinates are determined by the values of the function $B(x_i')$ and its derivative $B'(x_i')$ on the grid $\Omega_{x_i'}\{x_1' = x_0', \ldots, x_i', \ldots, x_N' = x_\varepsilon'\}$, found with the same accuracy accepted in the above chosen FEM scheme in the form of the power series of the small parameter $\varepsilon_n$:

$$B(x_i') = B_i^{(0)} + \sum_{k=1}^{k_{\max}} \frac{B_i^{(k)}(\varepsilon_n^{(1)}, \ldots, \varepsilon_n^{(k)})}{\rho^k},$$

$$B'(x_i') = b_i^{(0)} + \sum_{k=1}^{k_{\max}} \frac{b_i^{(k)}(\varepsilon_n^{(1)}, \ldots, \varepsilon_n^{(k)})}{\rho^k}, \quad (32)$$

using the Runge–Kutta method, in which all terms contain the power $k_{\max} + 1$ of $1/\rho$ and the higher powers are neglected. The expansion coefficients $B_i^{(k)} \equiv B_i^{(k)}(x_i')$ and $b_i^{(k)} \equiv b_i^{(k)}(x_i')$, calculated at the grid nodes $x_i'$ for the BVP (27) with the potential $\bar{V}(x')$ defined in Eq. (7) are presented in Fig. 6. One can see that in the vicinity of the potential well the corrections to the eigenfunctions are small, but at large $x'$ they become essential. The coefficient $b_i^{(0)}$, the derivative of the wave function with $\varepsilon_n = 0$, exponentially tends to a constant for $x' > 5.5$. From these observations the condition for choosing $x_\varepsilon$ follows. However, to avoid analytical calculations of the exponentially small terms in the effective potentials (21) between the weakly bound cluster states and pseudostates, it is sufficient to choose $x_\varepsilon' = 10$.

The interval $\varphi_0 \leq \varphi \leq \pi/2$ is divided into two subintervals by the point $\varphi_\varepsilon = x_\varepsilon/\rho$: $\varphi_0 < \varphi \leq \varphi_\varepsilon$ and $\pi/2 > \varphi > \varphi_\varepsilon$. In the calculations the point $x_\varepsilon$ was chosen from the condition $|V(x' > x_\varepsilon)| < \varepsilon$, where $\varepsilon > 0$ is a preassigned number, and the left-hand boundary of the interval $\varphi_0 = 0$. In the case of a high barrier, at the pair collision point, when the eigenfunctions in its vicinity are close to zero, the left boundary of the interval changes, $\varphi_0 = x_0'/\rho > 0$. The eigenfunctions $\phi_j(\varphi; \rho)$ are calculated in the form

$$\phi_j(\varphi; \rho) = \begin{cases} A_j(\rho) B_j(\varphi; \rho), & \varphi_0 \leq \varphi \leq \varphi_\varepsilon, \\ C_j(\rho) D_j^\sigma(\varphi; \rho), & \varphi_\varepsilon < \varphi \leq \pi/2, \end{cases} \quad (33)$$

$$2 \int_{\varphi_0}^{\pi/2} d\varphi (\phi_j(\varphi; \rho))^2 = 1. \quad (34)$$

Here $A_j(\rho)$ and $C_j(\rho)$ are the normalization factors, $B(\varphi; \rho)$ is determined from the numerical solution $B(x)$ in Cartesian coordinates using the transformation $\varphi = x'/\rho$; for $g$ and $u$ states

$$D_j^g(\varphi; \rho) = \sqrt{\frac{2}{\pi}} \cos\left( \frac{\sqrt{\varepsilon_j(\rho)}}{x_\alpha} (\varphi - \pi/2) \right),$$

$$D_j^u(\varphi; \rho) = \sqrt{\frac{2}{\pi}} \sin\left( \frac{\sqrt{\varepsilon_j(\rho)}}{x_\alpha} (\varphi - \pi/2) \right).$$

*Remark 3.* To simplify the analytic calculations with Maple math software [65], we take sin() and cos() in Eq. (33) for odd and even asymptotic eigenfunctions, respectively, thereby determining the asymptotic behavior up to the sign and the factor $\sqrt{2}$. The sign of the asymptotic eigenfunctions is then determined by matching the asymptotic expressions

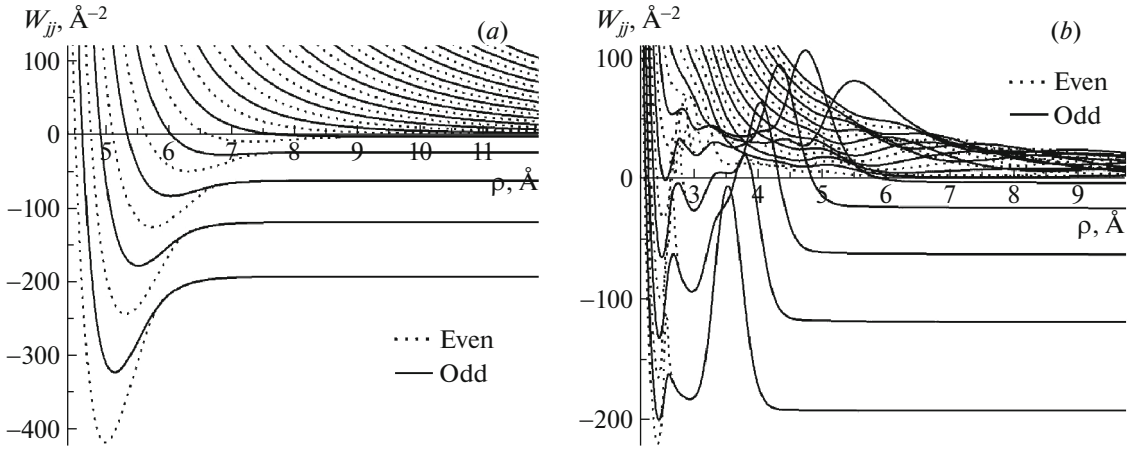


**Fig. 3.** The effective diagonal potentials $W_{jj}(\rho) = \varepsilon_j(\rho)\rho^{-2} + H_{jj}(\rho)$ for the $Be_3$ trimer $(a)$ and effective diagonal potentials $W_{jj}(\rho) = \varepsilon_j(\rho)\rho^{-2} + H_{jj}(\rho) + V^b_{jj}(\rho)$ for the tunneling problem of the dimer $Be_2$ through the Gaussian barrier $(b)$.

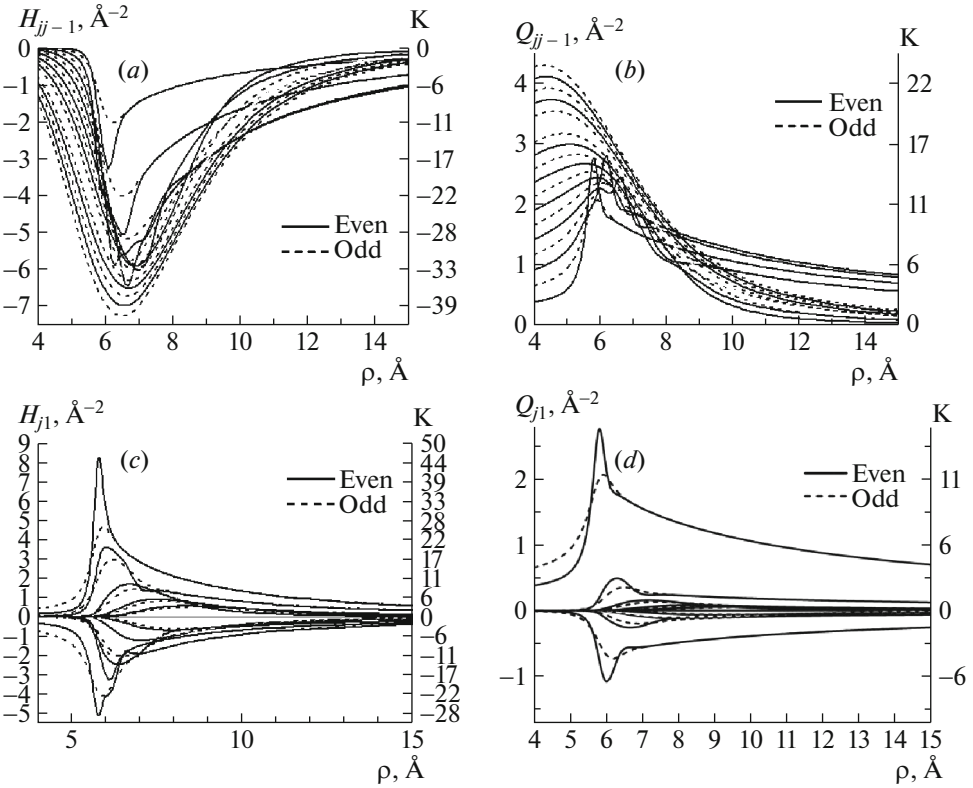


**Fig. 4.** The effective potentials (21) of $Be_3$: $(a)\ H_{jj-1}(\rho)$, $(b)\ Q_{jj-1}(\rho)$, $(c)\ H_{j1}(\rho)$, $(d)\ Q_{j1}(\rho)$. Here $j = 2, \ldots, 10$.

with the numerical values of eigenfunctions obtained by means of ODPEVP [52].

From the continuity of the eigenfunctions and their derivatives,

$$\phi_n(\varphi_\varepsilon - 0; \rho) = \phi_n(\varphi_\varepsilon + 0; \rho),$$
$$\frac{d\phi_n}{d\varphi}(\varphi_\varepsilon - 0; \rho) = \frac{d\phi_n}{d\varphi}(\varphi_\varepsilon + 0; \rho), \qquad (35)$$

we get the equation for the eigenvalue $\varepsilon_n(\rho)$:

$$\begin{cases} \tan\left(\frac{\sqrt{\varepsilon_n(\rho)}}{x_\alpha}(\varphi_\varepsilon - \frac{\pi}{2})\right) & \text{even } n \\ -\cot\left(\frac{\sqrt{\varepsilon_j(\rho)}}{x_\alpha}(\varphi_\varepsilon - \frac{\pi}{2})\right) & \text{odd } n \end{cases}$$
$$- \frac{\sqrt{\varepsilon_n(\rho)}}{x_\alpha R} = 0,$$

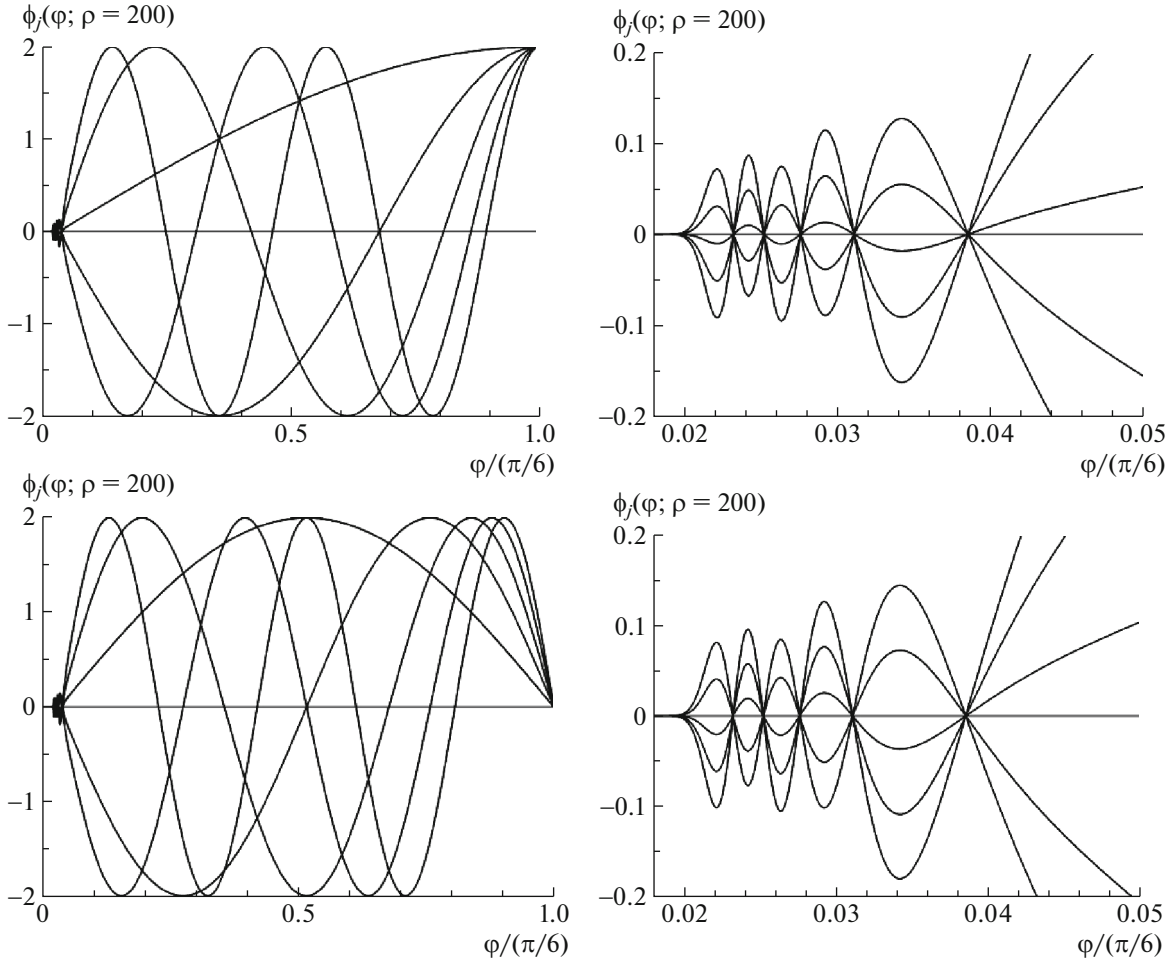


**Fig. 5.** The eigenfunctions $\phi_j(\varphi;\rho)$ corresponding to the eigenvalues $\varepsilon_j(\rho) \geq 0$ of the gerade ($g$) and ungerade ($u$) pseudostates $j = n + 1 = 6, \ldots, 10$ at $\rho = 200$.

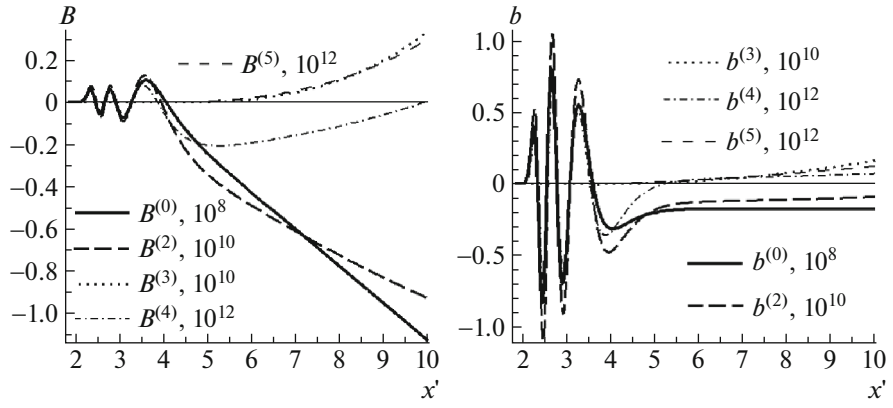


**Fig. 6.** The expansion coefficients $B^{(k)} \equiv B_i^{(k)}(\varepsilon_n^{(1)}, \ldots, \varepsilon_n^{(k)})$ and $b^{(k)} \equiv b_i^{(k)}(\varepsilon_n^{(1)}, \ldots, \varepsilon_n^{(k)})$, $k = 0, 2, 3, 4, 5$, at $n = 1$ with $\varepsilon_n^{(k)}$ given by Eq. (32) calculated at the nodes $x_i'$ of the grid $\Omega_{x'}$.

$$R = \frac{B_n'(\varphi_\varepsilon;\rho)}{B_n(\varphi_\varepsilon;\rho)} = \frac{\rho B_n'(x_\varepsilon)}{B_n(x_\varepsilon)}. \qquad (36)$$

Let us substitute (32) into (36), and then substitute (31) into the resulting equation. Expanding both sides of the equation in inverse powers of $\rho$, we arrive at the system of linear equations, from which the expansion coefficients $\varepsilon_n^{(k)}$, and then the coefficients $A_n(\rho)$ and $C_n(\rho)$ are determined.

Since the values of the function $B_n(\varphi;\rho)$ and its derivative $B'_n(\varphi;\rho)$ on the grid $\Omega_{\varphi;\rho}$ are known, we calculate the first integral using the quadrature formula of the Newton–Cotes type [64]. The second integral is calculated analytically using expansion (31). We have the analytical expression in the interval $\varphi_\varepsilon(\rho) < \varphi \le \pi/2$, and the explicit dependence of its values upon the parameter $\rho$ on the grid $\Omega_{\varphi;\rho}$. For the considered potential (7) and $n/\rho < 1$ we get the asymptotic expression (31) of the $g$ and $u$ potential curves at odd and even $n = j - n_0$, respectively. The first terms of these expansions are expressed as

$$\varepsilon_j^{(1)} = 4.4862257n^2, \quad \varepsilon_j^{(2)} = 15.094666n^2,$$
$$\varepsilon_j^{(3)} = -88.164324n^2 + 0.2988408n^4,$$
$$\varepsilon_j^{(4)} = -770.50344n^2 + 3.3516683n^4,$$
$$\varepsilon_j^{(5)} = -13803.854n^2 + 162.14850n^4 - 0.2922734n^6,$$
$$\varepsilon_j^{(6)} = -68926.763n^2 + 1584.0782n^4 - 4.4329308n^6$$

for the dimer, $x_\alpha = 1$, and

$$\varepsilon_j^{(1)} = 13.45867176n^2/9, \quad \varepsilon_j^{(2)} = 135.8518842n^2/9,$$
$$\varepsilon_j^{(3)} = (818.991555n^2 + 8.069491n^4)/9,$$
$$\varepsilon_j^{(4)} = (2179.34764n^2 + 271.51158n^4)/9,$$
$$\varepsilon_j^{(5)} = (-56227.6896n^2 + 9250.8082n^4 - 71.0683n^6)/9,$$
$$\varepsilon_j^{(6)} = (-1061661.971n^2 + 204829.893n^4 - 3233.746n^6)/9$$

for the trimer, $x_\alpha = 3$. The calculated eigenvalues in comparison with the numerical solution obtained by means of the program ODPEVP [52] are presented in Table 3. The described algorithm is implemented in the Maple–Fortran environment. The asymptotic expansions, obtained using it at $\rho = 50$, coincide with the numerical solution given by the FEM to 5–6 significant digits for the eigenvalues and to 4–5 significant digits for the eigenfunctions, see Table 3. The asymptotic expressions of the effective potentials (21) between the states $n_1 = i - n_0$ and $n_2 = j - n_0$ of the same ($g$ or $u$) parity at $n_0 = 5$, $i, j = n_0 + 1, \ldots$ for $n/\rho < 1$ have the form (see Appendix):

$$Q_{n_1n_2}(\rho) = \sum_{k=0}^{k_{\max}} \frac{Q_{n_1n_2}^{(k+2)}}{\rho^{k+2}},$$
$$H_{n_1n_2}(\rho) = \sum_{k=0}^{k_{\max}} \frac{H_{n_1n_2}^{(k+4)}}{\rho^{k+4}},$$
$$V_{n_1n_2}(\rho) = \sum_{k=0}^{k_{\max}} \frac{V_{n_1n_2}^{(k+1)}}{\rho^{k+1}}. \qquad (37)$$

Note, that in the matrix elements of barrier potentials (37) there are terms of the order $\rho^{-1}$ and $\rho^{-2}$ with positive and negative coefficients. This feature gives rise to a set of local minima (see Fig. 3*b*) that are important for the scattering problem under consideration and has the same nature as in the excited anti-protonic Helium atomcule [28].

Using Eqs. (29) and (33) we get the asymptotic expansions for $Q_{\text{in}}(\rho)$ and $H_{\text{in}}(\rho)$ between the cluster states $i = 1, \ldots, n_0$ and pseudostates $n - n_0 = 1, 2, \ldots$, for $n/\rho < 1$ (see Appendix):

$$Q_{\text{in}}(\rho) = \sum_{k=0}^{k_{\max}} \frac{Q_{\text{in}}^{(k+5/2)}}{\rho^{k+5/2}},$$
$$H_{\text{in}}(\rho) = \sum_{k=0}^{k_{\max}} \frac{H_{\text{in}}^{(k+7/2)}}{\rho^{k+7/2}},$$
$$V_{\text{in}}(\rho) = O(\exp(-\rho)). \qquad (38)$$

For *Task 2* and *Task 3*, expansions (29), (30) are the same, and expressions (37), (38) differ only in the numerical coefficients that were calculated above for *Task 3* on the interval $\varphi \in (0, \pi/2)$.

## 6. ASYMPTOTIC EXPRESSIONS OF FUNDAMENTAL SOLUTIONS

To calculate the asymptotic solution $\chi_{ii'}(\rho) \equiv \chi_{ii'}^{\sigma}(\rho)$ of the set of $N$ ODEs (19) at large values of the independent variable $\rho \ge \rho_{\max} \gg N$ ad we rewrite it in the form

$$\left[-\frac{1}{\rho^{d-1}}\frac{d}{d\rho}\rho^{d-1}\frac{d}{d\rho} + \mathcal{H}_{ii}(\rho) - E\right]\chi_{ii'}(\rho) = \sum_{j=1, j\ne i}^{N}\left[-Q_{ij}(\rho)\frac{d}{d\rho} - \frac{1}{\rho^{d-1}}\frac{d}{d\rho}\rho^{d-1}Q_{ij}(\rho) - H_{ij}(\rho)\right]\chi_{ji'}(\rho). \qquad (39)$$

The coefficients in Eq. (39) at $d = 2$, presented as inverse power series (29), (30), (31), (37), (38), have the form:

$$\mathcal{H}_{ii}(\rho) = \begin{cases} \varepsilon_i^{(0)} + \mathcal{H}_{ii}^{(2)}/\rho^2 + \sum\limits_{k=4} \mathcal{H}_{ii}^{(k)}/\rho^k, \\ i = 1, \ldots, n_o, \\ \mathcal{H}_{ii}^{(2)}/\rho^2 + \sum\limits_{k=3} \mathcal{H}_{ii}^{(k)}/\rho^k \\ i = n_o + 1, \ldots, \end{cases}$$

**Table 2.** The coefficients $\varepsilon_j^{(k)}$ and $H_{jj}^{(k)}$ in Å$^{-2}$ of expansions (29) and (30), and the comparison of $\sum\limits_{k=0}^{10} \varepsilon_j^{(k)}/\rho^k$ with the numerical values of $\varepsilon_j(\rho)$ for the dimer ($\varphi_\alpha = \pi/2$) or trimer ($\varphi_\alpha = \pi/6$) at $\rho = 20$ Å

| | | | | | |
|---|---|---|---|---|---|
| $\varepsilon_j^{(0)}$ | −193.06601252 | −119.39267226 | −63.338854932 | −24.904560537 | −4.0897890782 |
| $\varepsilon_j^{(2)}$ | −127.73059638 | −317.30568182 | −408.25519644 | −385.66879485 | −223.26092504 |
| $\varepsilon_j^{(4)}$ | −215.85831875 | −672.02680456 | −1198.7991074 | −1892.8857386 | −3079.0060449 |
| $\varepsilon_j^{(6)}$ | −667.46086524 | −2093.0917304 | −3656.2842793 | −5140.5360777 | −3803.8470973 |
| $\varepsilon_j^{(8)}$ | −2590.0140097 | −8317.9479477 | −15062.850569 | −23930.063302 | −63419.196580 |
| $\varepsilon_j^{(10)}$ | −11287.527768 | −37281.527942 | −69636.528276 | −107755.44601 | 164277.292590 |
| $\sum\limits_{k=0}^{10} \varepsilon_j^{(k)}/\rho^k$ | −193.38669866 | −120.19016966 | −64.367043142 | −25.880644327 | −4.6672470749 |
| $\varepsilon_j(\rho, \varphi_\alpha = \pi/2)$ | −193.38669866 | −120.19016966 | −64.367043142 | −25.880644327 | −4.6672471622 |
| $\varepsilon_j(\rho, \varphi_\alpha = \pi/6)$ | −193.38669866 | −120.19016966 | −64.367043142 | −25.880644327 | −4.6672471630 |
| $H_{jj}^{(2)}$ | 127.98059638 | 317.55568182 | 408.50519643 | 385.91879484 | 223.51081140 |
| $\varepsilon_j^{(2)} + H_{jj}^{(2)}$ | 0.2499999984 | 0.2499999944 | 0.2499999948 | 0.2499999953 | 0.2498863674 |

**Table 3.** Convergence of the expansion (31) for $\varepsilon_n(\rho)$ in Å$^{-2}$ $n = 1, 3, 5, 7$ (gerade) and $n = 2, 4, 6, 8$ (ungerade) at $\rho = 50$ Å and the numerical results (NUM) for the dimer

| | Gerade ($g$-parity) | | | | Ungerade ($u$-parity) | | | |
|---|---|---|---|---|---|---|---|---|
| $n^2$ | 1.000000 | 9.00000 | 25.00000 | 49.00000 | 4.000000 | 16.00000 | 36.000000 | 64.0000 |
| $+\varepsilon_n^{(1)}/\rho$ | 1.089724 | 9.80752 | 27.24311 | 53.39650 | 4.358898 | 17.43559 | 39.230082 | 69.7423 |
| $+\varepsilon_n^{(2)}/\rho^2$ | 1.095762 | 9.86186 | 27.39405 | 53.69235 | 4.383049 | 17.53219 | 39.447445 | 70.1287 |
| $+\varepsilon_n^{(3)}/\rho^3$ | 1.095059 | 9.85570 | 27.37792 | 53.66353 | 4.380266 | 17.52152 | 39.425152 | 70.0934 |
| $+\varepsilon_n^{(4)}/\rho^4$ | 1.094936 | 9.85464 | 27.37517 | 53.65878 | 4.379781 | 17.51968 | 39.421409 | 70.0877 |
| $+\varepsilon_n^{(5)}/\rho^5$ | 1.094893 | 9.85428 | 27.37437 | 53.65775 | 4.379613 | 17.51911 | 39.420448 | 70.0868 |
| $+\varepsilon_n^{(6)}/\rho^6$ | 1.094888 | 9.85425 | 27.37432 | 53.65774 | 4.379597 | 17.51906 | 39.420407 | 70.0868 |
| (NUM) | 1.094887 | 9.85424 | 27.37431 | 53.65776 | 4.379592 | 17.51905 | 39.420408 | 70.0869 |

$$H_{ij}(\rho) = \begin{cases} \sum\limits_{k=2} H_{ij}^{(k)}/\rho^k, & i,j = 1,\ldots,n_o, \\ \sum\limits_{k=4} H_{ij}^{(k)}/\rho^k, & i,j = n_o+1,\ldots, \\ \sum\limits_{k=7/2} H_{ij}^{(k)}/\rho^k, & \text{otherwise}, \end{cases}$$

$$Q_{ij}(\rho) = \begin{cases} \sum\limits_{k=1} Q_{ij}^{(k)}/\rho^k, & i,j = 1,\ldots,n_o, \\ \sum\limits_{k=2} Q_{ij}^{(k)}/\rho^k, & i,j = n_o+1,\ldots, \\ \sum\limits_{k=5/2} Q_{ij}^{(k)}/\rho^k, & \text{otherwise}. \end{cases}$$

The coefficients in these expansions can be determined by comparing Eqs. (39) and Eqs. (19) with the asymptotic expansions found in the previous section: $\mathcal{H}_{ii}^{(k)} = \varepsilon_i^{(k)} + H_{ii}^{(k)}$, $k = 2, 4, 6, \ldots$, $\mathcal{H}_{ii}^{(k)} = 0$, $k = 1, 3, 5, \ldots$, while $\mathcal{H}_{nn}^{(2)} = x_\alpha^2 n^2$, $\mathcal{H}_{nn}^{(3)} = \varepsilon_n^{(1)}$, $\mathcal{H}_{nn}^{(k)} = \varepsilon_n^{(k-2)} + H_{nn}^{(k)}$, $k = 4, 5, 6, \ldots$

**Step 1**. We express the desired solution of Eq. (39) in the form:

$$\chi_{ji'}(\rho) = \left(\phi_{ji'}(\rho) + \psi_{ji'}(\rho)\frac{d}{d\rho}\right) R_{i'}(\rho), \qquad (40)$$

where $\phi_{ji'}(\rho)$ and $\psi_{ji'}(\rho)$ are unknown functions, $R_{i'}(\rho)$ is a known function. We choose $R_{i'}(\rho)$ as fundamental solutions of the auxiliary problem treated as an etalon equation:

$$\left[-\frac{1}{\rho^{d-1}}\frac{d}{d\rho}\rho^{d-1}\frac{d}{d\rho} + \sum_{k=1}^{k'_{\max}} \frac{Z_{i'}^{(k)}}{\rho^k} - p_{i'}^2\right]$$

**Table 4.** The sets of the first resonance energy values $E$ at which the minimum of the transmission coefficient $|S_{ab}|^2_{ii}$ is achieved, the number $i$ of the threshold $\varepsilon_i$, the real and imaginary part of the complex energy eigenvalues $E_\nu = \Re E^M_\nu + \imath \Im E^M_\nu$ in Å$^{-2}$ of the even $g$ and odd $u$ metastable states of $Be_3$ numbered by index $\nu$ calculated with $N = 15$ equations (19)

| $E$ | $i$ | $\lvert S_{ab}\rvert^2_{ii}$ | $\Re E^M_\nu$ | $\Im E^M_\nu$ | $\nu$ type |
|---|---|---|---|---|---|
| −193.066 | 1 | | | | thr |
| −189.676 | 1 | $1 \times 10^{-7}$ | −188.94 | $-4 \times 10^{-2}$ | $1g$ |
| −164.654 | 1 | $4 \times 10^{-6}$ | −164.72 | $-1 \times 10^{-2}$ | $1u$ |
| −156.882 | 1 | $3 \times 10^{-6}$ | −157.04 | $-2 \times 10^{-2}$ | $2g$ |
| −140.545 | 1 | $1 \times 10^{-4}$ | −140.57 | $-5 \times 10^{-3}$ | $2u$ |
| −132.485 | 1 | $1 \times 10^{-6}$ | −132.47 | $-4 \times 10^{-3}$ | $3g$ |
| −124.256 | 1 | $1 \times 10^{-3}$ | −124.16 | $-6 \times 10^{-3}$ | $3u$ |
| −120.638 | 1 | $1 \times 10^{-6}$ | −120.75 | $-8 \times 10^{-2}$ | $4g$ |
| −119.392 | 2 | | | | thr |
| −113.248 | 2 | 0.10 | −113.24 | $-2 \times 10^{-2}$ | $5g$ |
| −89.319 | 2 | $9 \times 10^{-4}$ | −89.16 | $-3 \times 10^{-2}$ | $6g$ |
| −77.271 | 2 | 0.77 | −76.51 | $-4 \times 10^{-6}$ | $4u$ |
| −70.309 | 2 | 0.35 | −70.30 | $-2 \times 10^{-3}$ | $7g$ |
| −63.385 | 2 | 0.41 | −65.14 | $-3 \times 10^{-4}$ | $5u$ |
| −63.338 | 3 | | | | thr |
| −42.858 | 3 | 0.06 | −42.87 | $-6 \times 10^{-3}$ | $8g$ |
| −29.396 | 3 | 0.13 | −29.19 | $-4 \times 10^{-2}$ | $9g$ |
| −24.899 | 3 | 0.19 | −25.82 | $-1 \times 10^{-3}$ | $6u$ |
| −24.904 | 4 | | | | thr |
| −6.799 | 4 | 0.40 | −7.12 | $-1 \times 10^{-3}$ | $10g$ |
| −4.089 | 5 | | | | thr |

$$\times R_{i'}(\rho) = 0. \quad (41)$$

For example, for *Task 2* or *Task 3* we can choose $Z^{(2)}_{i'} = \mathcal{H}^{(2)}_{i'i'} = \varepsilon^{(2)}_{i'} + H^{(2)}_{ii} = 1/4$ at $i' = 1, \ldots, n_o$. Then the fundamental solutions $R_{i'}(\rho)$ are determined by the Hankel functions of the first and the second kind [64] $H^{(1,2)}_{1/2}\left(\sqrt{E - \varepsilon^{(0)}_j}\rho\right)$ at $E - \varepsilon^{(0)}_j > 0$ with the half-integer index $1/2$, $j = 1, \ldots, n_0$, and the corresponding Kelvin functions $K_{1/2}\left(\sqrt{\varepsilon^{(0)}_j - E}\rho\right)$ at $\varepsilon^{(0)}_j - E > 0$, $j = 1, \ldots, n_0$, in the closed channels. For *Task 2* we can choose $Z^{(2)}_{i'} = \mathcal{H}^{(2)}_{nn} = \varepsilon^{(2)}_n = x^2_\alpha(n - n_0)^2$ at $i' = n = n_o + 1, \ldots$ and $\varepsilon_j(\rho)\rho^{-2} \approx x^2_\alpha(j - n_0)^2\rho^{-2}$ for pseudostates. The fundamental solutions $R_{i'}(\rho)$ are Hankel functions of the first and the second kind [64] $H^{(1,2)}_m(\sqrt{E}\rho)$ at $E > 0$ with the integer index $m = x_\alpha(j - n_0) = 1x_\alpha, 2x_\alpha, \ldots$ in the open channels.

*Remark 4.* For *Task 3* at $E > 0$ in open channels at $i, i' = n_o + 1, \ldots,$ one should redefine $\mathcal{H}^{(k)}_{ii'} = \mathcal{H}^{(k)}_{ii'} + V^{(k)}_{ii'}$, where coefficients $V_{ii'}$ are coefficients of expansion (37), and the repulsive Coulomb-like term $Z^{(1)}_{i'}/\rho$ determined by diagonal matrix elements of Gaussian barrier potentials $Z^{(1)}_{i'} = V^{(1)}_{i'i'}$ in Eq. (41), and recalculate the above value of the coefficient $Z^{(2)}_{i'}$ of centrifugal terms $Z^{(2)}_{i'}/\rho^2$, i.e., $Z^{(2)}_{i'} \simeq V^{(2)}_{i'}$, using the diagonal $V^{(2)}_{i'i'}$ and nondiagonal $V^{(1)}_{i'i'}$ matrix elements of Gaussian barrier potentials from

Appendix. Then one should calculate the fundamental solutions in terms of the irregular and regular Coulomb functions [66] $R_{i'}(\rho) = (G_\nu(\sqrt{E}\rho) \pm \imath F_\nu(\sqrt{E}\rho))/\left(2\sqrt{\sqrt{E}\rho}\right)$ with real-valued indexes $\nu = \sqrt{Z_{i'}^{(2)}}$.

**Step 2**. At this step we calculate the coefficients $\phi_{i'}(\rho)$ and $\psi_{i'}(\rho)$ of expansion (40) in the form of truncated expansion in inverse powers of $\rho$ ($\phi_{ji'}^{(k'<0)} = \psi_{ji'}^{(k'<0)} = 0$):

$$\phi_{ji'}(\rho) = \phi_{ji'}^{(0)} + \sum_{k'} \frac{\phi_{ji'}^{(k')}}{\rho^{k'}},$$

$$\psi_{ji'}(\rho) = \psi_{ji'}^{(0)} + \sum_{k'} \frac{\psi_{ji'}^{(k')}}{\rho^{k'}}. \qquad (42)$$

Here $k' = 1, 3/2, 2, 5/2, \ldots, k_{\max}$, where $k_{\max}$ is integer or half-integer.

After the substitution of (42) into Eq. (39) with the use of Eq. (41), we arrive at the set of recurrence relations for $k' \le k_{\max}$:

$$\left(\varepsilon_i^{(0)} - E + p_{i'}^2\right)\phi_{ii'}^{(k')} + \left(\varepsilon_i^{(1)} - Z_{i'}^{(1)}\right)\phi_{ii'}^{(k'-1)} - 2p_{i'}^2(k'-1)\psi_{ii'}^{(k'-1)} = -f_{ii'}^{(k')},$$

$$\left(\varepsilon_i^{(0)} - E + p_{i'}^2\right)\psi_{ii'}^{(k')} + 2(k'-1)\phi_{ii'}^{(k'-1)} + \left(\varepsilon_i^{(1)} - Z_{i'}^{(1)}\right)\psi_{ii'}^{(k'-1)} = -g_{ii'}^{(k')}, \qquad (43)$$

where the right-hand sides $f_{ii'}^{(k')}$ and $g_{ii'}^{(k')}$ are defined by the expressions

$$f_{ii'}^{(k')} = -(k'-2)(k'-d)\phi_{ii'}^{(k'-2)} + \sum_{k=2}^{k'}\left(V_{ii}^{(k)} - Z_{i'}^{(k)}\right)\phi_{ii'}^{(k'-k)} + \sum_{k=1}^{k'}\left(Z_{i'}^{(k)}(2k'-2-k)\psi_{ii'}^{(k'-k-1)} + \sum_{j=1,j\neq i}^{N}\left(\sum_{k''=1}^{k'} 2Q_{ij}^{(k)} Z_{i'}^{(k'')}\psi_{ji'}^{(k'-k-k'')} - 2p_{i'}^2 Q_{ij}^{(k)}\psi_{ji'}^{(k'-k)} + Q_{ij}^{(k)}(-2k'+k+d+1)\phi_{ji'}^{(k'-k-1)} + V_{ij}^{(k)}\phi_{ji'}^{(k'-k)}\right)\right),$$

$$g_{ii'}^{(k)} = -(k'-1)(k'-3+d)\psi_{ii'}^{(k'-2)} + \sum_{k=2}^{k'}\left(V_{ii}^{(k)} - Z_{i'}^{(k)}\right)\psi_{ii'}^{(k'-k)} + \sum_{j=1,j\neq i}^{N}\sum_{k=1}^{k'}\Big(2Q_{ij}^{(k)}\phi_{ji'}^{(k'-k)} - Q_{ij}^{(k)}(2k'+d-3-k)\psi_{ji'}^{(k'-k-1)} + V_{ij}^{(k)}\psi_{ji'}^{(k'-k)}\Big) \qquad (44)$$

with the initial conditions $\phi_{ii'}^{(0)} = \delta_{ii'}$, $\psi_{ii'}^{(0)} = 0$ and $p_{i'}^2 = E - \varepsilon_{i'}^{(0)} \ge 0$ for open channels and $q_{i'}^2 = -p_{i'}^2 = \varepsilon_{i'}^{(0)} - E \ge 0$ for closed channels, $p_{i'} = \imath q_{i'}$, at $E < 0$ and $p_{i'} = \sqrt{E} > 0$ in open channels at $E > 0$, see *Remark 2*. Also from Eq. (43) at $k' = 1$ and $i = i'$,

$$\left(\varepsilon_{i'}^{(1)} - Z_{i'}^{(1)}\right)\phi_{i'i'}^{(0)} = 0,$$

$$\left(\varepsilon_{i'}^{(1)} - Z_{i'}^{(1)}\right)\psi_{i'i'}^{(0)} = 0, \qquad (45)$$

we obtain condition $Z_{i'}^{(1)} = V_{i'i'}^{(1)}$.

**Step 3.** Here we calculate the coefficients $\phi_{ii'}^{(k')}$ and $\psi_{ii'}^{(k')}$ using the step-by-step procedure of solving Eqs. (43) for $2E \neq \epsilon_{i'}^{(0)}$, $i \neq i'$ and $k' = 2, \ldots, k_{\max}$:

$$\phi_{ii'}^{(k')} = \left[\varepsilon_i^{(0)} - \varepsilon_{i'}^{(0)}\right]^{-1} \times \left[-f_{ii'}^{(k')} + 2p_{i'}^2(k'-1)\psi_{ii'}^{(k'-1)}\right],$$

$$\psi_{ii'}^{(k')} = \left[\varepsilon_i^{(0)} - \varepsilon_{i'}^{(0)}\right]^{-1}\left[-g_{ii'}^{(k')} - 2(k'-1)\phi_{ii'}^{(k'-1)}\right],$$

$$\phi_{mi'}^{(k'-1)} = -\left[2(k'-1)\right]^{-1} g_{mi'}^{(k')},$$

$$\psi_{mi'}^{(k'-1)} = \left[2(k'-1)\left(E - \varepsilon_{i'}^{(0)}\right)\right]^{-1} f_{mi'}^{(k')}. \qquad (46)$$

For $i' = 1, \ldots, n_0$ the subscripts $m$ and $i$ run $m = i'$, $i = 1, \ldots, n_0, n_0+1, \ldots$, $i \neq i'$, while for $i' = n_0 + 1, \ldots$, the subscripts $m$ and $i$ run $m = n_0+1, \ldots$, $i = 1, \ldots, n_0$.

The algorithm described above was implemented in MAPLE and FORTRAN to calculate the desired $\phi_{ii'}^{(k')}$ and $\psi_{ii'}^{(k')}$ up to the needed order $k_{\max}$.

The choice of the appropriate value $\rho_{\max}$ for the constructed expansions of the linearly independent solutions $\chi_{ji_o}$ for $p_{i_o} > 0$ is controlled by the fulfilment of the Wronskian condition to the prescribed accuracy:

$$Wr(\mathbf{Q}(\rho); \boldsymbol{\chi}^*(\rho), \boldsymbol{\chi}(\rho)) = \frac{4\imath}{\pi}\mathbf{I}_{oo},$$

$$Wr(\mathbf{Q}, \boldsymbol{\chi}^*, \boldsymbol{\chi}) \equiv \rho\left(\boldsymbol{\chi}^{*T}\left(\frac{d\boldsymbol{\chi}}{d\rho} - \mathbf{Q}\boldsymbol{\chi}\right)\right.$$

$$- \boldsymbol{\chi}^T \left( \frac{d\boldsymbol{\chi}^*}{d\rho} - \mathbf{Q}\boldsymbol{\chi}^* \right) \Big), \qquad (47)$$

where $\mathbf{I}_{oo}$ is the unit matrix of dimension $N_o \times N_o$ in the separated $\sigma$ representation or $2N_o \times 2N_o$ in the coupled $(\gamma\beta)$ representation, the asterisk * denotes complex conjugation, the superscript $^T$ denotes matrix transposition, $\boldsymbol{\chi}^- = \boldsymbol{\chi}^*$, and $\boldsymbol{\chi}^+ = \boldsymbol{\chi}$.

As an example, we present the first few terms of expansions (42) of the asymptotic expressions of the fundamental solutions (40) found by means of the above algorithms

$$\phi^{(0)}_{i_0 i_0} = 1, \quad \psi^{(1)}_{j_2 i_0} = -\frac{2Q^{(1)}_{j_2 i_0}}{\varepsilon^{(0)}_{j_2} - \varepsilon^{(0)}_{i_0}},$$

$$\psi^{(1)}_{i_0 i_0} = \sum_{j_2} \frac{2Q^{(1)}_{i_0 j_2} Q^{(1)}_{j_2 i_0}}{\varepsilon^{(0)}_{j_2} - \varepsilon^{(0)}_{i_0}} - \frac{\mathcal{H}^{(2)}_{i_0 i_0}}{2(E - \varepsilon^{(0)}_{i_0})}, \qquad (48)$$

$$\phi^{(2)}_{j_4 i_0} = -\frac{4(E - \varepsilon^{(0)}_{i_0}) Q^{(1)}_{j_4 i_0}}{(\varepsilon^{(0)}_{j_4} - \varepsilon^{(0)}_{i_0})} \sum_{j_2} \frac{Q^{(1)}_{i_0 j_2} Q^{(1)}_{j_2 i_0}}{(\varepsilon^{(0)}_{j_2} - \varepsilon^{(0)}_{i_0})}$$
$$- \frac{4(E - \varepsilon^{(0)}_{i_0})}{(\varepsilon^{(0)}_{j_4} - \varepsilon^{(0)}_{i_0})} \sum_{j_2} \frac{Q^{(1)}_{j_4 j_2} Q^{(1)}_{j_2 i_0}}{(\varepsilon^{(0)}_{j_2} - \varepsilon^{(0)}_{i_0})} - \frac{H^{(2)}_{j_4 i_0}}{\varepsilon^{(0)}_{j_4} - \varepsilon^{(0)}_{i_0}}$$
$$- \frac{Q^{(1)}_{j_4 i_0}((-4 - \mathcal{H}^{(2)}_{i_0 i_0})\varepsilon^{(0)}_{i_0} + 4E + \mathcal{H}^{(2)}_{i_0 i_0}\varepsilon^{(0)}_{j_4})}{(\varepsilon^{(0)}_{j_4} - \varepsilon^{(0)}_{i_0})^2}, \qquad (49)$$

$$\psi^{(5/2)}_{n_5 i_0} = -\frac{2Q^{(5/2)}_{n_5 i_0}}{\varepsilon^{(0)}_{n_5} - \varepsilon^{(0)}_{i_0}}. \qquad (50)$$

One can see that the desired compatibility conditions are proved and the Jacobi variables can be approximated as $y = \sqrt{\rho^2 - x^2} \approx \rho(1 - x^2/(2\rho^2) + \ldots)$ similar to [27, 30] in $\Psi_{i_o}(\rho, \varphi) \approx \sqrt{\rho}\Phi_{i_o}(x')\chi_{i_o i_o}(p_{i_o}, \rho(1 - x^2/(2\rho^2) + \ldots))$ at $i_o = 1, \ldots, n_o$ for cluster states below the breakup threshold. However, for pseudostates in open channels $i_o = n_o + 1, \ldots,$ above the breakup threshold we have other asymptotic expressions $\Psi_{i_o}(\rho, \varphi) \approx \sum_j \Phi_j(x')\chi_{j i_o}(\rho)$.

## 7. ASYMPTOTIC EXPRESSIONS OF SCATTERING, METASTABLE, AND BOUND STATES

The general solution $F_j$ of the system of ODEs in the open channels $i_o = 1, \ldots, N_o$ is determined by a linear combination of the fundamental solutions $\chi^-_{j i'_o}(p_{i_o}\rho)$ and $\chi^+_{j i'_o}(p_{i_o}\rho)$ calculated using Eqs. (40) and (48) with the leading terms of the Hankel functions of the first and the second kind in the form of incoming and outgoing waves

$$F^{\text{as}}_j(\rho) = \sum_{i'_o=1}^{N_o} \left[ \chi^-_{j i'_o}(p_{i_o}\rho) a^-_{i'_o} + \chi^+_{j i'_o}(p_{i_o}\rho) a^+_{i'_o} \right].$$

The scattering matrix $S^\sigma_{i_o i'_o}(E)$ or $S^\sigma_{i_o i'_o}(p)$, where $p = \text{diag}\{p_{i_o}\}_{i_o=1}^{N_o}$, is a diagonal matrix [22]. In open channels it is defined as the matrix transforming the amplitudes of the incoming waves $a^-_{i'_o}$ into those of the outgoing waves $a^+_{i'_o}$ [67]

$$a^+_{i'_o} = \sum_{i'_o=1}^{N_o} S^\sigma_{i_{o'} i_o}(p) a^-_{i_o}. \qquad (51)$$

The components of the radial asymptotic solutions $F^{\text{as}}_{j i_o}(\rho)$ of the scattering problem in the open channels $i_o = 1, \ldots, N_o$ have the form

$$F^{\text{as}}_{j i_o}(\rho)$$
$$= \sum_{i'_o=1}^{N_o} \left[ \chi^-_{j i'_o}(p_{i_o}\rho)\delta_{j i'_o} + \chi^+_{j i'_o}(p_{i_o}\rho) S^\sigma_{i'_o i_o}(p) \right], \quad (52)$$

while in the closed channel $i_o = N_o + 1, \ldots, N$ the asymptotic solutions $F_{j i_o}(\rho)$ are determined by the fundamental solutions $\chi^+_{j i'_o}(\imath p_i \rho)$, calculated using Eqs. (40) and (48) with the leading term of Kelvin functions $K_{1/2}(q^{(0)}_{i_o}\rho)$ for the decaying waves

$$F^{\text{as}}_{j i_o}(\rho) = a^+_{i'_o} \chi^+_{j i'_o}(\imath p_{i_o}\rho). \qquad (53)$$

These asymptotic solutions $\mathbf{F}(\rho) = \{\mathbf{F}_{i_o}(\rho)\}_{i_o=1}^N = \{\{F_{j i_o}(\rho)\}_{j=1}^N\}_{i_o=1}^N$ are used to have the conventional asymptotic boundary conditions for the components of the numerical solution $F_{j i_o}(\rho)$ of the system of ODEs (19) at large $\rho = \rho_{\max}$

$$F_{j i_o}(\rho) = F^{\text{as}}_{j i_o}(\rho),$$
$$\frac{d}{d\rho} F_{j i_o}(\rho) = \frac{d}{d\rho} F^{\text{as}}_{j i_o}(\rho). \qquad (54)$$

The scattering problem (3)–(6) with the asymptotic boundary conditions (52) and (53) is reduced to a boundary-value problem for the set of close-coupled equations (19) with the boundary conditions at $\rho = \rho_{\min}$ and $\rho = \rho_{\max}$ [56]:

$$\mathbf{F}(\rho_{\min}) = 0, \quad \left. \frac{d\mathbf{F}(\rho)}{d\rho} \right|_{\rho=\rho_{\max}}$$
$$= \mathcal{R}(\rho_{\max})\mathbf{F}(\rho_{\max}), \qquad (55)$$

where $\mathcal{R}(\rho_{\max})$ is a $N \times N$ symmetric matrix function of $E$, $\mathbf{F}(\rho) = \{\boldsymbol{\chi}_{i_o}(\rho)\}_{i_o=1}^N = \{\{\chi_{j i_o}(\rho)\}_{j=1}^N\}_{i_o=1}^N$ is the required $N \times N$ numerical matrix solution.

These matrices and the $N_o \times N_o$ matrices $\mathbf{S}_{\pm 1} = \{S^{g,u}_{i'_o i_o}(E)\}^{N_o}_{i'_o,i_o=1}$ sought for in the open channels $N_o = \max\limits_{E \geq \varepsilon_j} j \leq N$. are calculated directly from (54) using the program KANTBP 4M [57].

For metastable states the even and odd eigenfunctions obey the boundary conditions of the third kind (55), where the matrices $\mathcal{R}(\rho_{\max}) = \mathrm{diag}(\mathcal{R}(\rho_{\max}))$ depend on the complex energy eigenvalue $E \equiv E_m = \Re E_m + \imath \Im E_m$, $\Im E_m < 0$ sought for, and are expressed as [41]

$$\mathcal{R}_{i_o i_o}(\rho_{\max}) = \begin{Bmatrix} \imath p_m, & \Re E_m \geq \varepsilon^\sigma_j, \\ \imath q_m, & \Re E_m < \varepsilon^\sigma_j \end{Bmatrix},$$
$$p_m = \sqrt{E_m - \varepsilon^\sigma_{i_o}}, \quad q_m = \imath\sqrt{\varepsilon^\sigma_{i_o} - E_m}, \qquad (56)$$

since the asymptotic solutions of this problem contain only outgoing waves in the open channels $i_o = 1, \ldots, N_o$ and closed ones $i_o = N_o + 1, \ldots, N$. In this case the eigenfunctions obey the orthogonality and normalization conditions

$$(\mathbf{F}_m|\mathbf{F}_{m'}) = (\imath p_m + \imath p_{m'}) \times \left[\int\limits_{\rho_{\min}}^{\rho_{\max}} \mathbf{F}^T_m(\rho)\mathbf{F}_{m'}(\rho)d\rho - \delta_{mm'}\right] + C_{mm'} = 0,$$
$$C_{mm'} = -\mathbf{F}^T_m(\rho_{\max})\mathbf{F}_{m'}(\rho_{\max}) \qquad (57)$$

compatible with the conventional one [68].

For bound states the even ($g$) and odd ($u$) eigenfunctions obey the boundary conditions (55), with the matrices $\mathcal{R}(\rho_{\max}) = \mathrm{diag}(\mathcal{R}(\rho_{\max})) = 0$. In this case the eigenfunctions obey the orthogonality and normalization conditions

$$\langle \mathbf{F}_m|\mathbf{F}_{m'}\rangle = \int\limits_{\rho_{\min}}^{\rho_{\max}} \mathbf{F}^T_m(\rho)\mathbf{F}_{m'}(\rho)d\rho = \delta_{mm'}.$$

Taking the property (15) and (16) of the quasiangular parametric basis functions and the effective potentials (23) into account, we express the S-matrix in the $(\gamma\beta)$ representation on the full axis $\mathcal{R}^1$ via the matrix $S^\sigma$ (51), (52) calculated on the half-axis $\mathcal{R}^1_+$. The matrix $\mathbf{S}$ is a unitary and symmetric scattering matrix

$$\mathbf{S} = \begin{pmatrix} \mathbf{S}_{\gamma\gamma} & \mathbf{S}_{\gamma\beta} \\ \mathbf{S}_{\beta\gamma} & \mathbf{S}_{\beta\beta} \end{pmatrix}, \quad \mathbf{S}^\dagger\mathbf{S} = \mathbf{S}\mathbf{S}^\dagger = \mathbf{I}, \qquad (58)$$

consisting of the matrices $\mathbf{S}_{\gamma\gamma}$, $\mathbf{S}_{\beta\beta}$ and $\mathbf{S}_{\gamma\beta} = \mathbf{S}^T_{\gamma\beta}$ of the dimension $N_o \times N_o$ determined by the relations

$$\mathbf{S}_{\gamma\gamma} = \mathbf{S}_{\beta\beta} = (\mathbf{S}_{+1} + \mathbf{S}_{-1})/2,$$
$$\mathbf{S}_{\gamma\beta} = \mathbf{S}^T_{\beta\gamma} = (\mathbf{S}_{+1} - \mathbf{S}_{-1})/2, \qquad (59)$$

where $\mathbf{S}_{+1} \equiv \mathbf{S}_g$ and $\mathbf{S}_{-1} \equiv \mathbf{S}_u$ are the matrices from (52). Here $\mathbf{I}$ is the unit matrix with the dimension $2N_o \times 2N_o$, $\mathbf{S}_{\gamma\gamma}$ and $\mathbf{S}_{\beta\beta}$ correspond to the elastic scattering processes (in the considered case of 1D scattering it means reflection) of the dimer $(\alpha\beta)$ or $(\gamma\alpha)$ on the atom $\gamma$ (or $\beta$): $\gamma + (\alpha\beta) \to \gamma + (\alpha\beta)$, or $(\gamma\alpha) + \beta \to (\gamma\alpha) + \beta$, and $\mathbf{S}_{\beta\gamma}$ and the matrices $\mathbf{S}_{\gamma\beta}$ correspond to the inelastic rearrangement scattering processes (in the case of 1D scattering it means transmission) $\gamma + (\alpha\beta) \to (\gamma\alpha) + \beta$ or $(\gamma\alpha) + \beta \to \gamma + (\alpha\beta)$, for which the conventional relations between inelastic and elastic scattering below breakup threshold at $E < 0$ follow from (58) that provide conservation of the Wronskian (47), $|\mathbf{S}_{\beta\gamma}|^2 = \mathbf{I} - |\mathbf{S}_{\gamma\gamma}|^2$ and $\mathbf{S}_{\beta\gamma} = \mathbf{S}^T_{\gamma\beta}$, where $\mathbf{I}$ is the unit $N_o \times N_o$ matrix. The incoming (outgoing) wave of rearrangement scattering $\gamma + (\alpha\beta) \to (\gamma\alpha) + \beta$ or $(\gamma\alpha) + \beta \to \gamma + (\alpha\beta)$ propagates along the corresponding $y_{(\alpha\beta)\gamma}$ ($y_{(\gamma\alpha)\beta}$) or $y_{(\gamma\alpha)\beta}$ ($y_{(\alpha\beta)\gamma}$) axis in the backward or forward direction (see Fig. 1*b*). For example, in the first sector of Fig. 1*b* the incident wave of the rearrangement scattering $3 + (12) \to (31) + 2$ or $(31) + 2 \to 3 + (12)$ propagates in the channel $3 + (12)$ or $(31) + 2$ along the corresponding $y_{(12)3} > 0$ axis at $x_{12} > 0$ or $y_{(31)2} < 0$ axis at $x_{31} > 0$ in the backward or forward direction, while the outgoing wave propagates in the channel $3 + (12)$ or $(31) + 2$ along the corresponding $y_{(31)2} < 0$ axis at $x_{31} > 0$ or $y_{(12)3} > 0$ axis at $x_{12} > 0$ in the backward or forward direction. It means that the states $\gamma$ and $\beta$ of the scattering matrix $\mathbf{S}_{\beta\gamma} = \mathbf{S}^T_{\gamma\beta}$ of the direct and inverse rearrangement scattering processes $\gamma + (\alpha\beta) \to (\gamma\alpha) + \beta$ and $(\gamma\alpha) + \beta \to \gamma + (\alpha\beta)$ have different signs of velocities with respect to the corresponding Jacobi vectors connecting the atom and the dimer in both ingoing and outgoing channels.

For the scattering of the dimer $(\gamma\beta)$ by the potential barriers, considered on the full axis, the matrix $\mathbf{S}$ is the $2N_o \times 2N_o$ scattering matrix (58) read as similar to [41]

$$\mathbf{S} = \begin{pmatrix} \mathbf{R}_{\leftarrow} & \mathbf{T}_{\rightarrow} \\ \mathbf{T}_{\leftarrow} & \mathbf{R}_{\rightarrow} \end{pmatrix}, \quad \mathbf{S}^\dagger\mathbf{S} = \mathbf{S}\mathbf{S}^\dagger = \mathbf{I}, \qquad (60)$$

where $\mathbf{I}$ is the unit matrix with the dimension $2N_o \times 2N_o$ consisting of the amplitudes of the reflected and transmitted waves $\mathbf{R}_v = \mathbf{R}_v(E)$ and $\mathbf{T}_v = \mathbf{T}_v(E)$, where $v = \leftarrow, \rightarrow$ indicates the direction of the incident wave propagation with respect to the $y$ axis, i.e., $v = \leftarrow$ and $v = \rightarrow$ for $y > 0$ and $y < 0$, respectively, and the $N_o \times N_o$ matrices $\mathbf{R}_v = \mathbf{R}_v(E)$ and $\mathbf{T}_v = \mathbf{T}_v(E)$ are expressed as

$$\mathbf{R}_{\leftarrow} = \mathbf{R}_{\rightarrow} = (\mathbf{S}_{+1} + \mathbf{S}_{-1})/2,$$

$$\mathbf{T}_{\leftarrow} = \mathbf{T}_{\rightarrow}^{T} = (\mathbf{S}_{+1} - \mathbf{S}_{-1})/2. \quad (61)$$

For the scattering of the dimer $(\alpha\beta)$ on potential barriers similar relations determine the reflection $\mathbf{R}_{\leftarrow} = \mathbf{S}_{\gamma\gamma}$ and $\mathbf{R}_{\rightarrow} = \mathbf{S}_{\beta\beta}$, and transmission $\mathbf{T}_{\leftarrow} = \mathbf{S}_{\beta\gamma}$ and $\mathbf{T}_{\rightarrow} = \mathbf{S}_{\gamma\beta}$ amplitudes. For the reflection coefficient $|\mathbf{R}_v|^2 = \mathbf{R}_v^{\dagger}\mathbf{R}_v$ and the transmission coefficient $|\mathbf{T}_v|^2 = \mathbf{T}_v^{\dagger}\mathbf{T}_v$ the conventional relation below breakup threshold at $E < 0$ following from (58) and constant wronskian (47), $|\mathbf{T}_v|^2 = \mathbf{I} - |\mathbf{R}_v|^2$ is valid, where $\mathbf{I}$ is the unit $N_o \times N_o$ matrix.

## 8. BOUND, METASTABLE, AND SCATTERING STATES OF THE TRIMER

For the considered models, the eigenvalues and the hyperradial components of 2D eigenfunctions of the BVP for the set of ODEs (19) with Dirichlet boundary conditions were calculated with the predetermined accuracy using the FEM implemented in the KANTBP 4M program [57].

The set of even $(g)$ and odd $(u)$ bound states of the trimer $Be_3$ (*Task 2*) were calculated on the grid $\Omega_h = \{\rho_{\min} = 4.24(1)4.33(10)6.13(1)6.33(23)\rho_{\max} = 11.39\}$, where in parentheses the number of the fifth-order Hermitian elements [55] is indicated, for the number of equations $N = 15$ in the system (19).

The set of binding energies of the trimer $Be_3$ is presented in Table 1, and the trimer eigenfunctions (11) are shown in Fig. 7. These solutions, i.e. the real eigenvalues and the corresponding eigenfunctions, were used as an initial approximation in the continuous analog of Newton's method [28] with additional condition $(\mathbf{F}_m|\mathbf{F}_{m'}) = 0$ to calculate the metastable states of the trimer $Be_3$ on the same finite-element grid. The corresponding problem of the dimer scattering on an atom was solved on the same grid and $N = 15$.

The calculated complex energies of the metastable states $E_m^M \equiv E_m = \Re E_m + i\Im E_m$ for the trimer are presented in Table 4. *These metastable states are responsible for the resonance energies, corresponding to the minimal probability of inelastic scattering of the dimer by the atom, i.e., to the resonance quantum reflection from the potential well (Feshbach resonances, see Figs. 1b and 3a).*

As an example, in Fig. 8 we display the eigenfunctions of the scattering problem for gerade and ungerade states corresponding to the minimum of the transmission coefficient $|S_{\gamma\beta}|^2 = |S_{\beta\gamma}|^2 = 10^{-7}$ at $E = -189.676$, as well as the metastable state 1g from Table 4. The isolines of the absolute values $|\Psi^{\gamma,\beta}(y,x)|$ of the linear combinations $\Psi^{\gamma,\beta}(y,x) = (\Psi^g(y,x) \pm \Psi^u(y,x))/\sqrt{2}$ demonstrate the effect of the resonance reflection from the effective potential well. It can be seen from the figures that the shape of the wave functions of the gerade scattering states (Fig. 8*a*) and metastable states (Fig. 9) are similar and they are localized in the vicinity of the potential well (Fig. 3*a*). At the same time, for the same energy value $E = -189.6$ Å$^{-2}$, the wave function of ungerade scattering states (Fig. 8*b*) is a typical nonresonant wave function.

## 9. METASTABLE AND SCATTERING STATES OF THE DIMER TUNNELING

The metastable states of the dimer $Be_2$ tunneling through Gaussian barriers of *Task 3* were calculated for BVP calculated with $N = 15$ equations in the system (19) with matrix elements of the potential barrier on the finite element grid $\Omega_\rho = \{\rho_{\min} = 1.81(12)4.21(15)\rho_{\max} = 7.51\}$ with the fifth-order Hermitian elements $(p = 5)$. The corresponding problem of a dimer tunneling through the barriers was solved on the same grid.

The corresponding algebraic eigenvalue problem for metastable states was solved using the above mentioned continuous analogue of Newton's method. As the initial approximation the real eigenvalues and the corresponding orthonormalized eigenfunctions (58) were used. They were found as a result of solving the bound state problem with $\mathcal{R}(y^t) = 0$ on the grid $\Omega_\rho = \{\rho_{\min} = 1.81(12)\rho_{\max} = 4.21\}$. The complex values of energy of the metastable states $E_m^M \equiv E_m = \Re E_m + i\Im E_m$ for the dimer $Be_2$ tunneling through the Gaussian barriers, are presented in Fig. 10. *These metastable states are responsible for the resonance values of energy, corresponding to the maximal transmission coefficient, i.e., the quantum transparency of the potential barriers (see Figs. 1b and 3b), i.e., the shape resonances.* The position of peaks presented in Fig. 10 is seen to be in quantitative agreement with the real part $\Re(E)$, and the geometric halfwidth of the $|T|_{11}^2(E)$ peaks agrees by the order of magnitude with the imaginary part $\Gamma = -2\Im(E)$ of the complex energy eigenvalues $E = \Re(E) + i\Im(E)$ of the metastable states. The obtained complex energy values corresponding to the resonance values of energy in the first open channel are in good agreement with the ones calculated analytically in the model of a rigid diatomic molecule with Morse potential tunneling trough the Gaussian barrier at the same values of parameters [13]. From Fig. 10 one can see that as the energy of the initial excited state increases, the transmission peaks demonstrate a shift towards higher energies, the set of peak positions keeping approximately the same as for the transitions from the ground state, and the peaks just replace each other.

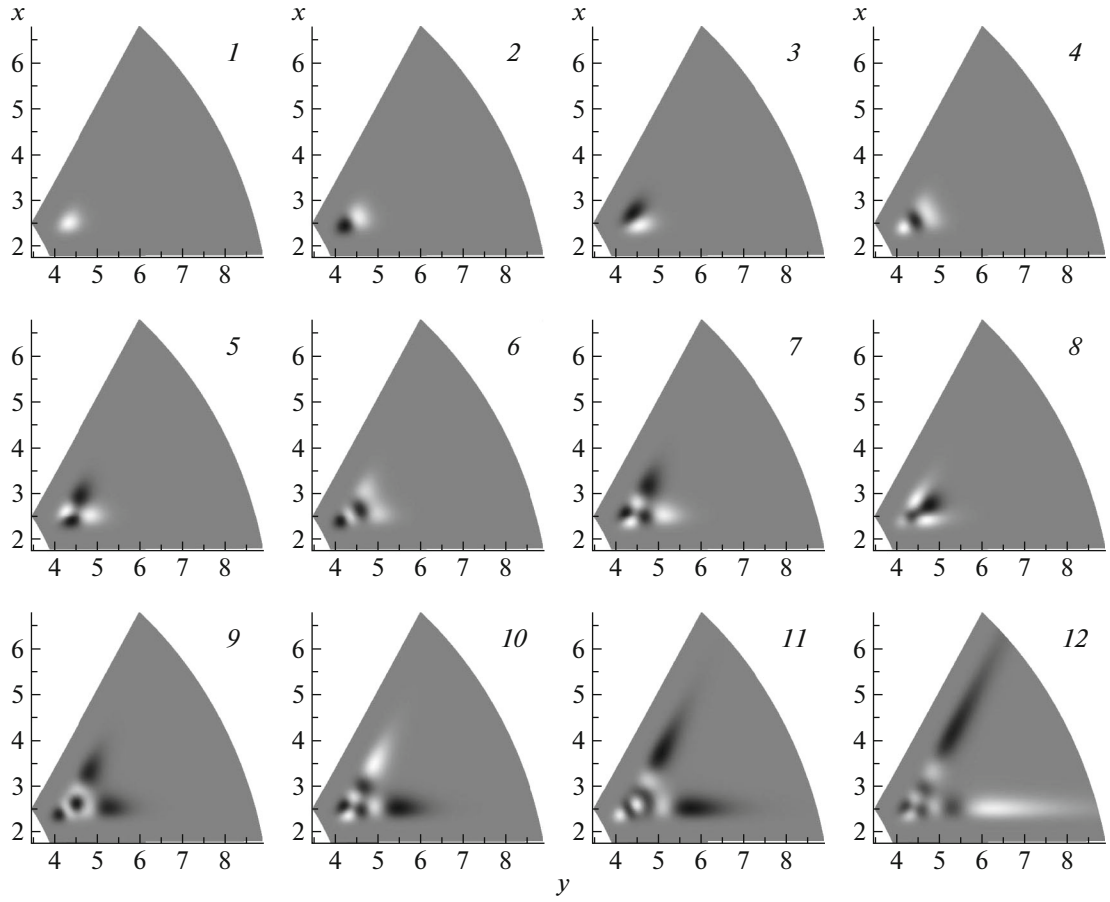


**Fig. 7.** The density plots of the eigenfunctions $\Psi_\nu^{g,u}(\varphi,\rho)$ displayed in sector 1 of $(y,x)$ plane (in Å) of the gerade $(g)$ and ungerade $(u)$ bound states with energies $E_\nu^{g,u}$ of the $Be_3$ trimer presented in Table 1. The negative, positive, and near-zero values of the eigenfunctions are displayed by black, white, and gray, respectively.

For example, the left epure shows that the positions of the 13th and 14th peaks for the transitions from the first state coincide with the positions of the 1st and 2nd peaks for the transitions from the second state, while the right epure shows that the positions of the 25th and 26th peaks for transitions from the first state coincide with the positions of the 13th and 14th peaks for transitions from the second state and with the positions of the 1st and 2nd peaks for the transitions from the third state.

For a quantum particle, the possibility of tunneling makes the concept of potential barrier activation ill-defined and, therefore, deviations from Arrhenius behavior may be expected. Diffusion can still be approximately described in this form by using a temperature-dependent activation energy, often much lower than the classical energy barrier, i.e., the effective barrier for two noninteracting atoms is $2\tilde{V}_0$. The normalized thermal rate constant $\hat{k}^{qn}/k_{(0)}^{qn}$ has the form [29, 69, 70]:

$$\hat{k}^{qn}/k_{(0)}^{qn} = \sum_{i=1}^{N_o} \hat{k}_i(T), \quad \hat{k}_i(T) = \frac{e^{-\tilde{\varepsilon}_i/T}}{Q_{vib}} k_i(T),$$

$$Q_{vib} = \sum_{i=1}^{N_o} e^{-\tilde{\varepsilon}_i/T}, \tag{62}$$

$$k_i(T) = \frac{1}{\sqrt{T}} \int\limits_0^{\tilde{E}_y^{\max}} W_{ii}(\tilde{E}_y) e^{-\tilde{E}_y/T} d\tilde{E}_y$$

$$+ \frac{1}{\sqrt{T}} \int\limits_{\tilde{E}_y^{\max}}^{\infty} W_{ii}(\tilde{E}_y) e^{-\tilde{E}_y/T} d\tilde{E}_y, \tag{63}$$

where $\hat{k}_i(T)$ are the weighed thermal rate constants, $Q_{vib}$ is the vibrational energy and $k_i(T)$ is the partial thermal rate constant in the initial vibrational state $i$, $W_{ii}(\tilde{E}) = |T|_{ii}^2(\tilde{E})$ is the total transmission probability for the initial state $i$. Figure 11$a$ illustrates the

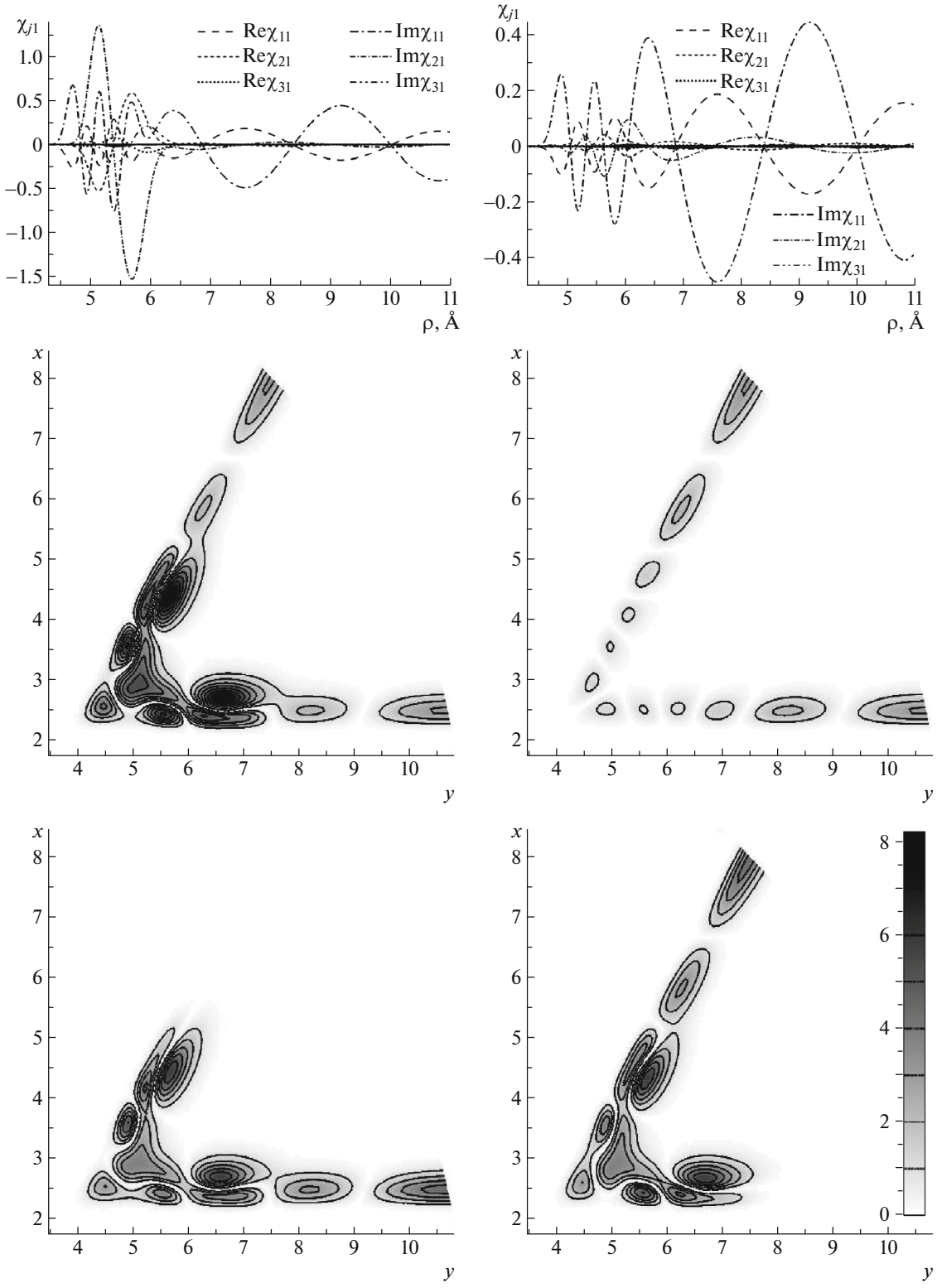


**Fig. 8.** Upper and middle panels: the gerade (left-hand panel) and ungerade (right-hand panel) solutions $\chi_{j1}(\rho)$ as functions of the hyperradius $\rho$ (Å) and isolines of the absolute values $|\Psi^{g,u}(\varphi,\rho)|$ of corresponding solutions in sector 1 of $(y,x)$ plane (in Å) for the scattering of Be atom with the energy $-E = 189.676$ Å$^{-2}$ (relative to the three-body threshold) on the dimer $Be_2$, corresponding to the 1g metastable state from Table 4. Lower panel: isolines of the absolute values $|\Psi^{\gamma,\beta}(\varphi,\rho)|$ of the linear combinations $\Psi^{\gamma,\beta}(\varphi,\rho) = (\pm\Psi^{u}(\varphi,\rho) + \Psi^{g}(\varphi,\rho))/\sqrt{2}$.

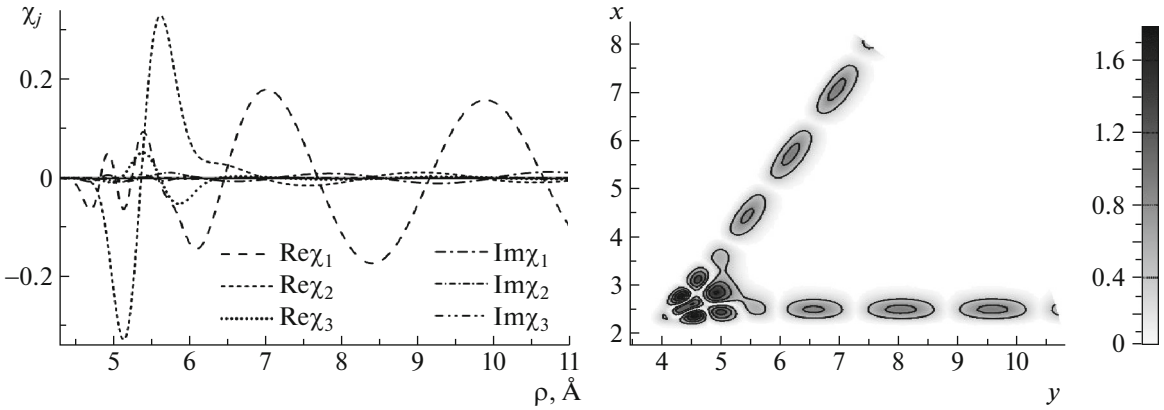


**Fig. 9.** The components $\chi_j$ and isolines of the absolute values $|\Psi(\varphi,\rho)|$ of the solution $\Psi(\varphi,\rho)$ for the trimer $Be_3$ in 1g metastable state with the real part of energy eigenvalues $\Re E = -188.94$ Å$^{-2}$, localized near the minima of the trimer potential.

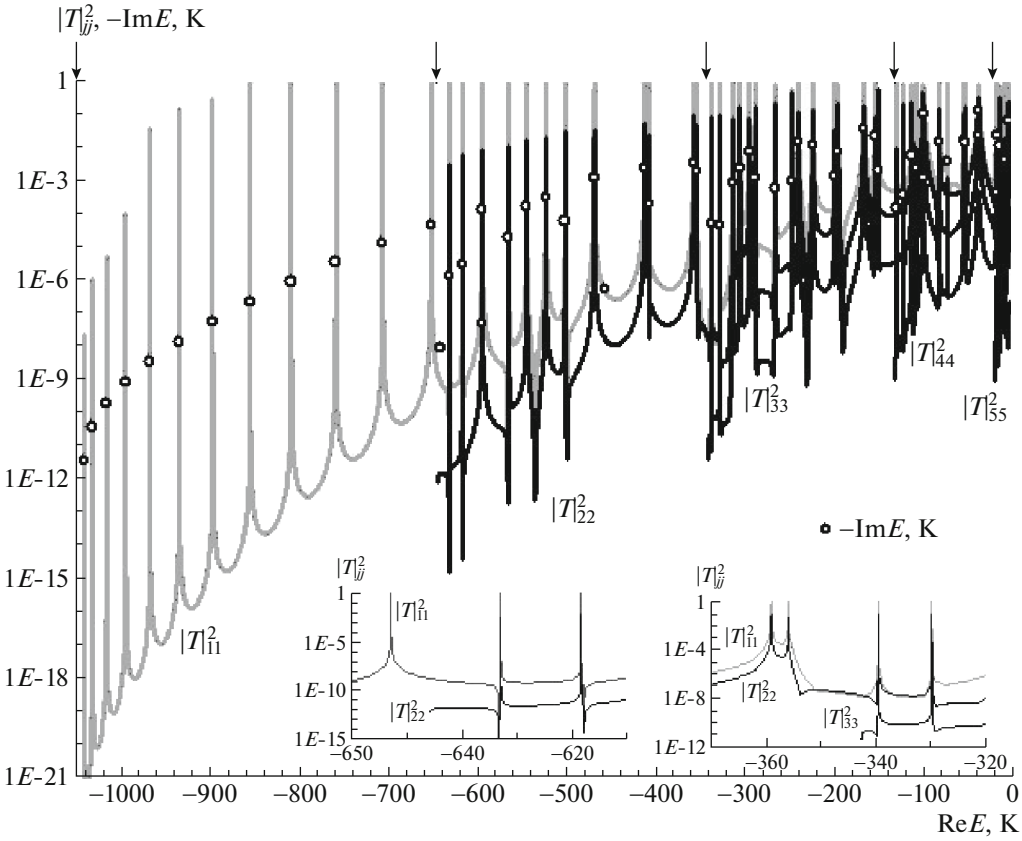


**Fig. 10.** The total probability $|\mathbf{T}|^2_{ii}(E) = \sum_{j=1}^{N_o} T^*_{ij}T_{ji}$ (lines) of penetration of the dimer for the initial states $i$ through the repulsive Gaussian potential barriers versus the total energy $E = \Re E$ counted from the main threshold $E = 0$. The values of the threshold energies $E = \varepsilon_i$, $i = 1,\ldots,5$ corresponding to the energies of ground and excited initial states are shown by arrows. The real $\Re E$ and imaginary $(-1)\Im E$ part (with negative sign) of the metastable states' energy (circles).

comparison of the partial $\hat{k}_i(T)$ (solid curve), weighed $k_i(T)$ (dashed lines) and total $k(T)$ (dash–dotted curve) thermal rate constants vs the temperature $T$ and their upper, lower, and average estimates.

The total $\hat{E}^a(T)$ and the partial $E^a_i(T)$ temperature-dependent activation energy is defined by

$$\hat{E}^a(T) = -\frac{1}{\sqrt{\beta}\hat{k}(T)}\frac{d\sqrt{\beta}\hat{k}(T)}{d\beta},$$

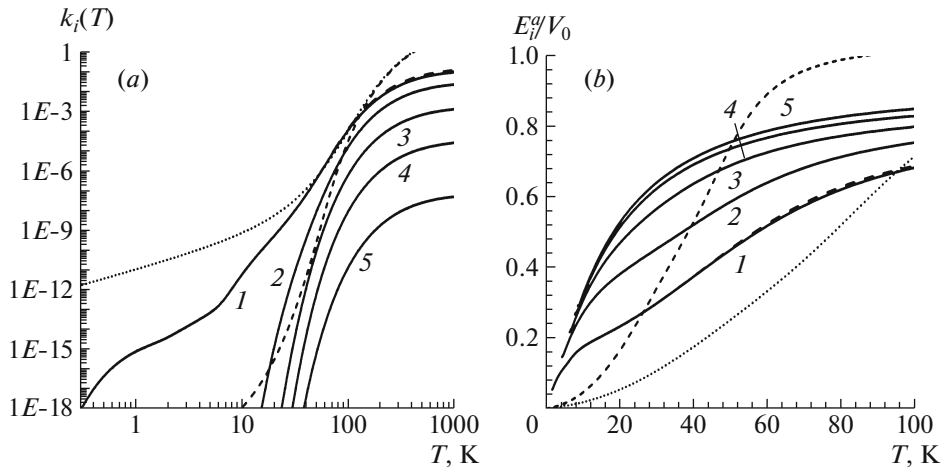


**Fig. 11.** ($a$) Thermal rate constants vs. temperature: partial $\hat{k}_i(T)$ (solid curves) and total $k(T)$ (long dashed curve) and their upper (dotted curve) and lower (short dashed curve) estimates. ($b$) The temperature-dependent activation energy: partial $E_i^a(T)/V_0$ (solid curves) and total $E^a(T)/V_0$ (long dashed curve) activation energy and its upper (short dashed curve) and lower (dotted curve) estimates.

$$E_i^a(T) = -\frac{1}{\sqrt{\beta}k_i(T)}\frac{d\sqrt{\beta}k_i(T)}{d\beta}, \quad \beta = 1/T.$$

Figure 11$b$ displays the comparison of the partial $E_i^a(T)$ (solid curve) and the total $\hat{E}^a(T)$ (dash–dotted curve) activation energy vs temperature $T$ and their upper, lower, and average estimates in the interval restricted by $T_{\max} = 100$ K. In terms of the quantum mechanical transition state theory [29, 69] it leads to the increased thermal rate constants of the quantum tunneling and decreased activation energy $E_i^a/V_0$ of the composite molecular system at the low temperature $T$ below the classical energy barrier $V_0$ (see Fig. 11).

## 10. CONCLUSION

The model for beryllium trimer in collinear configuration on a straight line was formulated as a 2D boundary-value problem for the Schrödinger equation in polar coordinates. Using the Kantorovich expansions this problem has been reduced to the boundary-value problem for a set of second-order ordinary differential equations.

The symbolic–numeric algorithms are proposed and implemented in Maple to evaluate the asymptotic expansions (29), (30), (31), (37), and (38) of the parametric BVP eigensolutions and the effective potentials $W_{ij}(\rho)$ in inverse powers of large values of the (hyper)radius $\rho$.

These expansions have been used for the calculation of the asymptotic expressions of the fundamental solutions (40) of the system of the second-order ODEs at large values of $\rho$ using recurrence relations (43) and construction of asymptotic states (52) and (53) of triatomic scattering problem both below and above the breakup threshold. It was shown that to solve tunneling of atomic dimer thought the short range potential barrier in open channels above the dissociation threshold of dimer at $E > 0$ the additional effective repulsive Coulomb-like term evidently arises as one can see from the linear dependence of $V^b(x, y)$ in the plane, see Fig. 1$d$ in the SODEs at large value of radial variable, as well as leading terms of expansions of diagonal and nondiagonal matrix elements of the Gaussian barrier potentials of second and first inverse power of the radial variable. In this case one must use in construction of the asymptotic scattering states instead of the Hankel functions of the first and second type the irregular and regular Coulomb functions with real valued indexes [66].

The effects of resonant quantum transmission of atomic dimers through the potential barrier and reflection from the effective potential well of a trimer, arising in the scattering process were revealed (see Figs. 3$a$ and 3$b$), generated by metastable states of the composite system (cluster + barrier or well) with complex energy eigenvalues below the dissociation threshold of dimer, corresponding to the shape and Feshbach resonances, respectively.

The proposed method of solving the three-atomic scattering problem as well as dimer tunneling through potential barrier in adiabatic representation both below and above breakup threshold can be applied to the further analysis of quantum transparency and reflection effects [13, 14, 44], quantum diffusion [29] and the resonance scattering in triatomic systems using modern theoretical and experimental results [9–12] and algorithms and programs [50, 52–54, 57]. It can be also applied in the studies of laser control of

molecular tunneling, aimed at enhancing the rate of chemical reactions and quantum diffusion [58] and ternary fission of heavy-ion collision in a collinear configuration [71, 72].

## ACKNOWLEDGMENTS

The authors thank Profs. V.P. Gerdt, S.B. Levin, A.V. Mitin, A.K. Motovilov, F.M. Pen'kov, V.V. Pupyshev, I.V. Puzynin, and Dr. L.L. Hai for useful discussions. The work was partially supported by the RFBR (grant no. 16-01-00080), the Bogoliubov–Infeld and Hulubei–Meshcheryakov programs, the MES RK (grant no. 0333/GF4) and grant of Plenipotentiary Representative of the Government of the Republic of Kazakhstan in the framework of collaboration program JINR–RK. The publication has been prepared with the support of the "RUDN University Program 5-100".

*Appendix*

## ASYMPTOTIC EXPRESSIONS OF MATRIX ELEMENTS FOR DIMER AND TRIMER

The first coefficients of the expansions (30) for both the dimer of *Tasks 3 and 1* and the trimer of *Task 2* have the form

$$Q_{ij}^{(1)} = \begin{pmatrix} 0 & 10.3201 & -3.81790 & 1.83170 & -0.903311 \\ -10.3201 & 0 & 12.2419 & -5.54402 & 2.68986 \\ 3.81790 & -12.2419 & 0 & 11.5096 & -5.30745 \\ -1.83170 & 5.54402 & -11.5096 & 0 & 7.99437 \\ 0.903311 & -2.68986 & 5.30745 & -7.99437 & 0 \end{pmatrix},$$

$$Q_{ij}^{(3)} = \begin{pmatrix} 0 & 19.6114 & -3.63427 & 1.58999 & -6.31271 \\ -19.6114 & 0 & 32.2355 & -12.5531 & 22.0625 \\ 3.63427 & -32.2355 & 0 & 52.0431 & -53.8134 \\ -1.58999 & 12.5531 & -52.0431 & 0 & 105.275 \\ 6.31271 & -22.0625 & 53.8134 & -105.275 & 0 \end{pmatrix},$$

$$Q_{ij}^{(5)} = \begin{pmatrix} 0 & 68.2366 & -6.68774 & -14.8770 & 128.505 \\ -68.2366 & 0 & 91.6918 & 27.6600 & -356.227 \\ 6.68774 & -91.6918 & 0 & 68.9065 & 595.104 \\ 14.8770 & -27.6600 & -68.9065 & 0 & -523.035 \\ -128.505 & 356.227 & -595.104 & 523.035 & 0 \end{pmatrix},$$

$$H_{ij}^{(2)} = \begin{pmatrix} 127.981 & -67.2820 & -85.3811 & 73.3913 & -44.4889 \\ -67.2820 & 317.556 & -161.487 & -40.5195 & 46.8714 \\ -85.3811 & -161.487 & 408.505 & -231.091 & 45.2520 \\ 73.3913 & -40.5195 & -231.091 & 385.919 & -215.798 \\ -44.4889 & 46.8714 & 45.2520 & -215.798 & 223.511 \end{pmatrix},$$

$$H^{(4)}_{ij} = \begin{pmatrix} 414.479 & -142.333 & -526.641 & 464.604 & -624.169 \\ -142.333 & 1204.00 & -420.171 & -812.366 & 1119.09 \\ -526.641 & -420.171 & 2009.09 & -947.285 & -464.551 \\ 464.604 & -812.366 & -947.285 & 3041.77 & -2605.05 \\ -624.169 & 1119.09 & -464.551 & -2605.05 & 5091.16 \end{pmatrix},$$

$$H^{(6)}_{ij} = \begin{pmatrix} 1912.47 & -670.689 & -2112.77 & 815.251 & 4153.61 \\ -670.689 & 5431.40 & -1689.40 & -3295.46 & -646.435 \\ -2112.77 & -1689.40 & 8482.51 & -2016.27 & -12077.1 \\ 815.251 & -3295.46 & -2016.27 & 10047.9 & 12431.9 \\ 4153.61 & -646.435 & -12077.1 & 12431.9 & -664.074 \end{pmatrix}.$$

The first terms of the expansions (37) for the dimer of *Tasks 3 and 1* are $Q^{\bullet}_{n_1n_2} = 2\hat{Q}^{\bullet}_{n_1n_2}$, $H^{\bullet}_{n_1n_2} = 2\hat{H}^{\bullet}_{n_1n_2}$, $V^{\bullet}_{n_1n_2} = 4\hat{V}^{\bullet}_{n_1n_2}$,

$$\hat{Q}^{(2)}_{n_1n_2} = 2.2431128\frac{n_1n_2}{(n_1^2-n_2^2)},$$

$$\hat{Q}^{(3)}_{n_1n_2} = 5.0315554\frac{n_1n_2}{(n_1^2-n_2^2)},$$

$$\hat{Q}^{(4)}_{n_1n_2} = 188.67822\frac{n_1n_2}{(n_1^2-n_2^2)} + 0.22413\frac{n_1n_2(n_1^2+n_2^2)}{(n_1^2-n_2^2)},$$

$$\hat{H}^{(4)}_{n_1n_2} = 10.06311\frac{n_1n_2(n_1^2+n_2^2)}{(n_1^2-n_2^2)^2},$$

$$\hat{H}^{(5)}_{n_1n_2} = 45.14538\frac{n_1n_2(n_1^2+n_2^2)}{(n_1^2-n_2^2)^2} + 69.93509n_1n_2,$$

$$\hat{H}^{(6)}_{n_1n_2} = -1642.273\frac{n_1n_2(n_1^2+n_2^2)}{(n_1^2-n_2^2)^2} + 8.044\frac{n_1^3n_2^3}{(n_1^2-n_2^2)^2} + 476.762n_1n_2,$$

$$\hat{H}^{(4)}_{n_1n_1} = 0.6289444 + 2.0691442n_1^2,$$

$$\hat{H}^{(5)}_{n_1n_1} = 2.8215867 + 79.217746n_1^2,$$

$$\hat{H}^{(6)}_{n_1n_1} = -102.642068 + 138.328874n_1^2 + 0.826991n_1^4.$$

The first terms of the expansions (37) for the dimer of *Task 3* have the form

$$\hat{V}^{(1)}_{ij} = 61.031\sin\frac{\pi n_1}{4}\sin\frac{\pi n_2}{4},$$

$$\hat{V}^{(2)}_{ij} = -107.521\left(n_1\sin\frac{\pi n_2}{4}\cos\frac{\pi n_1}{4} + n_2\cos\frac{\pi n_2}{4}\sin\frac{\pi n_1}{4}\right) + 136.900\sin\frac{\pi n_1}{4}\sin\frac{\pi n_2}{4},$$

$$\hat{V}^{(3)}_{ij} = -482.366\left(n_2\cos\frac{\pi n_2}{4}\sin\frac{\pi n_1}{4} + n_1\sin\frac{\pi n_2}{4}\cos\frac{\pi n_1}{4}\right) + 191.020n_1n_2\cos\frac{\pi n_2}{4}\cos\frac{\pi n_1}{4} - 95.510\sin\frac{\pi n_1}{4}\sin\frac{\pi n_2}{4}(n_1^2+n_2^2-3.21518)$$

$$\hat{V}^{(4)}_{ij} = -629.005\sin\frac{\pi n_1}{4}\times\sin\frac{\pi n_2}{4}(n_1^2+n_2^2+5.37240) + 1572.068\left(n_2\cos\frac{\pi n_2}{4}\sin\frac{\pi n_1}{4} + n_1\sin\frac{\pi n_2}{4}\cos\frac{\pi n_1}{4}\right) + 1285.443n_1n_2\cos\frac{\pi n_2}{4}\cos\frac{\pi n_1}{4} + 49.862\left(\cos\frac{\pi n_2}{4}\sin\frac{\pi n_1}{4}n_2^3 + \sin\frac{\pi n_2}{4}\cos\frac{\pi n_1}{4}n_1^3\right) + 171.075\left(\cos\frac{\pi n_2}{4}\sin\frac{\pi n_1}{4}n_1^2n_2 + \sin\frac{\pi n_2}{4}\cos\frac{\pi n_1}{4}n_1n_2^2\right).$$

The first terms of the expansions (37) for the trimer of *Task 2* are

$$\hat{Q}^{(2)}_{n_1n_2} = -6.729337\frac{n_1n_2}{(n_1^2-n_2^2)},$$
$$\hat{Q}^{(3)}_{n_1n_2} = 5.031555\frac{n_1n_2}{(n_1^2-n_2^2)},$$
$$\hat{H}^{(4)}_{n_1n_2} = 90.567936\frac{n_1n_2(n_1^2+n_2^2)}{(n_1^2-n_2^2)^2},$$
$$\hat{H}^{(5)}_{n_1n_2} = 1218.924228\frac{n_1n_2(n_1^2+n_2^2)}{(n_1^2-n_2^2)^2} + 1834.900654n_1n_2$$
$$\hat{H}^{(4)}_{n_1n_1} = 5.660496 + 18.622285n_1^2,$$
$$\hat{H}^{(5)}_{n_1n_1} = 76.182764 + 2085.531903n_1^2.$$

The first terms of the expansions (38) for the dimer of *Tasks 3 and 1* have the form $Q^{\bullet}_{1n} = \sqrt{2}(-1)^{[n/2]}\hat{Q}^{\bullet}_{1n}$, $H^{\bullet}_{1n} = \sqrt{2}(-1)^{[n/2]}\hat{H}^{\bullet}_{1n}$

$$\hat{Q}^{(5/2)}_{1n} = -0.428911n, \quad \hat{Q}^{(7/2)}_{1n} = -1.443145n, \quad \hat{Q}^{(9/2)}_{1n} = -25.01600n + 0.183791n^3,$$
$$\hat{Q}^{(5/2)}_{2n} = 1.273900n, \quad \hat{Q}^{(7/2)}_{2n} = +4.286254n, \quad \hat{Q}^{(9/2)}_{2n} = 75.66328n - 0.546657n^3,$$
$$\hat{Q}^{(5/2)}_{3n} = -2.497511n, \quad \hat{Q}^{(7/2)}_{3n} = -8.403301n, \quad \hat{Q}^{(9/2)}_{3n} = -152.3919n + 1.075421n^3,$$
$$\hat{Q}^{(5/2)}_{4n} = 3.668834n, \quad \hat{Q}^{(7/2)}_{4n} = +12.34441n, \quad \hat{Q}^{(9/2)}_{4n} = 231.9007n - 1.599005n^3,$$
$$\hat{Q}^{(5/2)}_{5n} = -4.098659n, \quad \hat{Q}^{(7/2)}_{5n} = -13.79066n, \quad \hat{Q}^{(9/2)}_{5n} = -247.9253n + 2.018873n^3,$$
$$\hat{H}^{(7/2)}_{1n} = 22.53006n, \quad \hat{H}^{(9/2)}_{1n} = +77.24936n, \quad \hat{H}^{(11/2)}_{1n} = 1551.8678n - 9.835892n^3,$$
$$\hat{H}^{(7/2)}_{2n} = -26.57543n, \quad \hat{H}^{(9/2)}_{2n} = -93.70381n, \quad \hat{H}^{(11/2)}_{2n} = -2203.032n + 11.89657n^3,$$
$$\hat{H}^{(7/2)}_{3n} = -12.19890n, \quad \hat{H}^{(9/2)}_{3n} = -32.64199n, \quad \hat{H}^{(11/2)}_{3n} = 262.11512n + 4.400493n^3,$$
$$\hat{H}^{(7/2)}_{4n} = 85.06821n, \quad \hat{H}^{(9/2)}_{4n} = +273.8820n, \quad \hat{H}^{(11/2)}_{4n} = 4387.8346n - 35.91925n^3,$$
$$\hat{H}^{(7/2)}_{5n} = -120.4823n, \quad \hat{H}^{(9/2)}_{5n} = -391.5948n, \quad \hat{H}^{(11/2)}_{5n} = -8001.428n + 54.83111n^3.$$

The first terms of the expansions (38) for the trimer of Task 2 are $Q^{\bullet}_{1n} = \sqrt{2}(-1)^{[n/2]}\hat{Q}^{\bullet}_{1n}$, $H^{\bullet}_{1n} = \sqrt{2}(-1)^{[n/2]}\hat{H}^{\bullet}_{1n}$

$$\hat{Q}^{(5/2)}_{1n} = -1.286735n, \quad \hat{Q}^{(7/2)}_{1n} = -12.988310n,$$
$$\hat{Q}^{(5/2)}_{2n} = 3.821702n, \quad \hat{Q}^{(7/2)}_{2n} = +38.576285n,$$
$$\hat{Q}^{(5/2)}_{3n} = -7.492536n, \quad \hat{Q}^{(7/2)}_{3n} = -75.629699n,$$
$$\hat{Q}^{(5/2)}_{4n} = 11.006506n, \quad \hat{Q}^{(7/2)}_{4n} = +111.099726n,$$
$$\hat{Q}^{(5/2)}_{5n} = 12.295975n, \quad \hat{Q}^{(7/2)}_{5n} = +124.116000n,$$
$$\hat{H}^{(7/2)}_{1n} = 67.590204n, \quad \hat{H}^{(9/2)}_{1n} = +12.988310n,$$
$$\hat{H}^{(7/2)}_{2n} = -79.726329n, \quad \hat{H}^{(9/2)}_{2n} = -38.576285n,$$
$$\hat{H}^{(7/2)}_{3n} = -36.596734n, \quad \hat{H}^{(9/2)}_{3n} = -75.629699n,$$
$$\hat{H}^{(7/2)}_{4n} = 255.204699n, \quad \hat{H}^{(9/2)}_{4n} = +111.099726n,$$
$$\hat{H}^{(7/2)}_{5n} = 361.447878n, \quad \hat{H}^{(9/2)}_{5n} = +124.116000n.$$

## REFERENCES


1. V. N. Efimov, Sov. J. Nucl. Phys. **12**, 589 (1971).
2. V. Efimov, Nature Phys. **5**, 533 (2009).
3. M. Zaccanti et al., Nature Phys. **5**, 586 (2009).
4. J. Voigtsberger et al., Nature Commun. **5**, 5765 (2014).
5. C. H. Greene, P. Giannakeas, and J. Pérez-Ríos, Rev. Mod. Phys. **89**, 035006 (2017).
6. E. A. Kolganova and A. K. Motovilov, Comput. Phys. Commun. **126**, 88 (2000).
7. M. Salci, S. Levin, N. Elander, and E. Yarevsky, J. Chem. Phys. **129**, 134304 (2008).
8. A. A. Korobitsin and E. A. Kolganova, Phys. Part. Nucl. **48**, 900 (2017).
9. J. M. Merritt, V. E. Bondybey, and M. C. Heaven, Science **324**, 1548 (2009).
10. K. Patkowski, V. Špirko, and K. Szalewicz, Science **326**, 1382 (2009).
11. A. V. Mitin, Int. J. Quantum Chem. **111**, 2560 (2011).
12. A. V. Mitin, Chem. Phys. Lett. **682**, 30 (2017).
13. P. M. Krassovitskiy and F. M. Pen'kov, J. Phys. B **47**, 225210 (2014).
14. S. I. Vinitsky et al., Lect. Not. Comp. Sci. **8660**, 472 (2014).
15. A. A. Gusev et al., Commun. Comp. Inf. Sci.**678**, 511 (2016).
16. S. I. Vinitskii and L. I. Ponomarev, Sov. J. Part. Nucl. **13**, 557 (1982).
17. P. P. Fiziev and Ts.Ya. Fizieva, Few-Body Systems **2**, 71 (1987).
18. R. T. Pack and G. A. Parker, J. Chem. Phys. **87**, 3888 (1987); G. A. Parker and R. T. Pack, **98**, 6883 (1993).
19. M. B. Kadomtsev, S. I. Vinitsky, and F. R. Yukajlovic, Phys. Rev. A **36**, 4652 (1987).
20. S. I. Vinitskii, S. P. Merkur'ev, I. V. Puzynin, and V. M. Suslov, Sov. J. Nucl. Phys. **51**, 406 (1990).
21. Yu. A. Kuperin et al., Ann. Phys. **205**, 330 (1991).
22. S. I. Vinitskiĭ, B. L. Markovski, and A. A. Suz'ko, Sov. J. Nucl. Phys. **55**, 371 (1992).

23. L. D. Faddeev and S. P. Merkuriev, *Quantum Scattering Theory for Several Particle Systems* (Kluwer Acad. Publ., Doderecht, 1993).
24. S. P. Merkur'ev, A. K. Motovilov, and S. D. Yakovlev, Theor. Math. Phys. **94**, 306 (1993).
25. V. V. Pupyshev, Phys. Part. Nucl. **30**, 689 (1999); **35**, 256 (2004).
26. O. Chuluunbaatar, A. A. Gusev, S. Y. Larsen, and S. I. Vinitsky, J. Phys. A **35**, L513 (2002).
27. O. Chuluunbaatar et al., J. Phys. B **39**, 243 (2006).
28. I. V. Puzynin et al., Phys. Part. Nucl. **38**, 70 (2007).
29. E. Pijper and A. Fasolino, J. Chem. Phys. **126**, 014708 (2007).
30. O. Chuluunbaatar et al., J. Phys. A **40**, 11485 (2007).
31. N. P. Mehta, B. D. Esry, and C. H. Greene, Phys. Rev. A **76**, 022711 (2007).
32. V. V. Pupyshev, Theor. Math. Phys. **155**, 862 (2008); *ibid*. **179**, 472 (2014); *ibid*. **193**, 1602 (2017).
33. E. A. Kolganova, V. Roudnev, and M. Cavagnero, arXiv:1010.1404v1 [physics.atm-clus].
34. V. S. Buslaev, S. B. Levin, P. Neittaannmäki, and T. Ojala, J. Phys. A: Math. Theor. **43**, 285205 (2010).
35. V. S. Buslaev, Ya.Yu. Koptelov, S. B. Levin, and D. A. Strygina, Phys. Atom. Nucl. **76**, 208 (2013).
36. A. M. Budylin and S. B. Levin, Zap. Nauchn. Sem. POMI **438**, 95 (2015) [J. Math. Sci. (N. Y.) **224** (1), 63 (2017)].
37. I. V. Baybulov, A. M. Budylin, and S. B. Levin, Zap. Nauchn. Sem. POMI **461**, 14 (2017).
38. P. A. Belov and S. L. Yakovlev, Phys. Atom. Nucl. **77**, 344 (2014).
39. V. V. Pupyshev, Phys. Atom. Nucl. **77**, 664 (2014).
40. A. A. Gusev et al., Phys. Atom. Nucl. **77**, 389 (2014).
41. A. A. Gusev et al., Theor. Math. Phys. **186**, 21 (2016).
42. A. A. Gusev, O. Chuluunbaatar, S. I. Vinitsky, and V. L. Derbov, Bull. Peoples' Friendship Univ. Russ. Ser. "Math. Inf. Sci. Phys.", No. 4, 56 (2016).
43. A. A. Gusev et al., Lect. Not. Comp. Sci. **10490**, 151 (2017).
44. A. A. Gusev et al., Acta Phys. Pol. B Proc. Suppl. **10**, 269 (2017).
45. V. V. Pupyshev, Theor. Math. Phys. **195**, 548 (2018); preprint JINR P4-2016-83.
46. L. V. Kantorovich and V. I. Krylov, *Approximate Methods of Higher Analysis* (Wiley, New York, 1964).
47. Z. A. Vlasova, Trudy Mat. Inst. Steklov. **53**, 16 (1959).
48. A. A. Gusev, O. Chuluunbaatar, S. I. Vinitsky, A. G. Abrashkevich, and V. L. Derbov, Math. Mod. Geom. **2**, 54 (2014).
49. S. Yu. Slavyanov, *Asymptotic Solutions of the One-dimensional Schrodinger Equation* (AMS, Providence, 1996).
50. O. Chuluunbaatar et al., Comput. Phys. Commun. **177**, 649 (2007); O. Chuluunbaatar et al., **179**, 685 (2008); A. A. Gusev et al., **185**, 3341 (2014).
51. S. I. Vinitsky et al., Progr. Comp. Soft. **33**, 105 (2007).
52. O. Chuluunbaatar, A. A. Gusev, S. I. Vinitsky, and A. G. Abrashkevich, Comput. Phys. Commun. **181**, 1358 (2009).
53. O. Chuluunbaatar, A. A. Gusev, S. I. Vinitsky, and A. G. Abrashkevich, Comput. Phys. Commun. **185**, 2636 (2014).
54. A. A. Gusev, O. Chuluunbaatar, S. I. Vinitsky, and A. G. Abrashkevich, Bull. Peoples' Friendship Univ. Russ. Ser. Math. Inf. Sci. Phys. **2**, 336 (2014).
55. A. A. Gusev, O. Chuluunbaatar, S. I. Vinitsky, et al., Lect. Not. Comp. Sci. **8660**, 138 (2014).
56. A. A. Gusev, O. Chuluunbaatar, S. I. Vinitsky, and A. G. Abrashkevich, Math. Mod. Geom. **3**, 22 (2015).
57. A. A. Gusev, L. L. Hai, O. Chuluunbaatar, S. I. Vinitsky, [`http://wwwinfo.jinr.ru/programs/jinrlib/kantbp4m`](2015).
58. M. Shapiro and P. Brumer, *Quantum Control of Molecular Processes* (Wiley-VCH, Weinheim, 2012).
59. J. Wang, G. Wang, and J. Zhao, J. Phys. Cond. Matt. **13**, L753 (2001).
60. L. J. Lauhon and W. Ho, Phys. Rev. Lett. **85**, 4566 (2000).
61. J. F. Cornwell, *Group Theory in Physics* (Academic Press, London, 1984).
62. F. A. Cotton, *Chemical Applications of Group Theory,* 3rd ed. (Wiley, New York 1990).
63. I. V. Komarov, L. I. Ponomarev, and S. Yu. Slavyanov, *Spheroidal and Coulomb Spheroidal Functions* (Nauka, Moskva, 1976) (in Russian).
64. M. Abramovits and I. A. Stegun, *Handbook of Mathematical Functions* (Dover, New York, 1972).
65. www.maplesoft.com.
66. A. R. Barnett, Comput. Phys. Commun. **24**, 141 (1981).
67. R. G. Newton, J. Math. Phys. **1**, 319 (1960); **2**, 188 (1961).
68. V. I. Kukulin, V. M. Krasnopolsky, and J. Horáček, *Theory of Resonances: Principles and Applications* (Springer, Netherlands, 1989).
69. W. H. Miller, J. Chem. Phys. **61**, 1823 (1974).
70. S. I. Vinitsky et al., Proc. SPIE **9031**, 90311E (2014).
71. Yu.V. Pyatkov et al., Phys. Atom. Nucl. **73**, 1309 (2010).
72. R. B. Tashkhodjaev et al., Phys. Rev. C **91**, 054612 (2015).